

Volume 13, 2018

ISSN 1314-6289

# **JOURNAL SCIENTIFIC AND APPLIED RESEARCH**



Association Scientific and Applied Research

*VOLUME 13, 2018*

***JOURNAL  
SCIENTIFIC AND APPLIED RESEARCH***



**Association Scientific and Applied Research**

**International Journal**

The journal publishes scientific information and articles which present new and unpublished results from research in the spheres of the mathematical, physical, chemical, natural, humanitarian, social, medical, Earth, forest and agricultural sciences.

Every article is to be read by two independent anonymous reviewers. After their acceptance and after the author presents a bank statement for the paid publishing fee, the article is published in the refereed JOURNAL SCIENTIFIC AND APPLIED RESEARCH, which is an academic journal licensed in **EBSCO**, USA.

**Editor – in - Chief:**

**Corr. Member Prof. DSc Petar Getsov – Director of Space Research  
and Technologies Institute – BAS Chairman of  
Bulgarian Astronautic Federation**

**Vice – Editor- in- Chief:**

**Prof. DSc Zhivko Zhekov - Association Scientific and Applied Research**

**International Editorial Board:**

Acad. Prof DSc Valery Bondur – Russia  
Acad. Prof. DSc Mykhailo Khvesyk – Ukraine  
Corr. Member Prof. DSc Filip Filipov – Bulgaria  
Prof. DSc Garo Mardirossian – Bulgaria  
Prof. DSc Olga Prokopenko – Ukraine  
Prof. DSc Andrei Andreev – Bulgaria  
Prof. DSc Borislav Bedzhev – Bulgaria  
Prof. Dr. Habil. Georgi Kolev – Bulgaria  
Prof. Dr. Rumen Nedkov – Bulgaria  
Prof. Dr. Dimitar Teodosiev – Bulgaria  
Prof. Dr. Stefan Zhelev – Bulgaria  
Assoc. Prof. Dr. Andrei Bogdanov – Bulgaria  
Assoc. Prof. Dr. Ognian Fetfov – Bulgaria  
Assoc. Prof. Dr. Hristo Krachunov – Bulgaria  
Ch. Assist. Prof. Dr. Petar Boyanov – Bulgaria  
Dr. Alen Sarkisyan – France  
Dr. Stoyan Sargoychev – Canada  
Chief Assist. Angel Manev – Bulgaria

**Editors**

Aneliya Karagyozyan– Bulgaria  
Assoc. Prof. Dr. Anton Antonov – Bulgaria

**Dek: TOPEX/POSEIDON altimeter data reveal our Ocean Planet, mission for NASA.**

© Association Scientific and Applied Research  
© Konstantin Preslavsky University Press  
ISSN 1314-6289  
zhekov\_z@abv.bg  
<http://rst-tto.com>

# CONTENTS

## Technical Sciences

---

### MODELING AND ANALYSIS OF THE "AIRPLANE-AUTOPILOT" SYSTEM IN DESCENDING ATMOSPHERIC DISTURBANCE

P. Getsov, D. Jordanov, WangBo, St. Getsov .....5

### QUASI-MONTE CARLO METHODS FOR COMPUTATION OF MULTIDIMENSIONAL INTEGRALS RELATED TO BAYESIAN MODELS IN INTERNATIONAL MIGRATION FORECASTING

Venelin Todorov, Valentin Dimitrov, Iliyan Tsvetkov, Yuri Dimitrov.....13

### A NUMERICAL STUDY ON QUASI MONTE CARLO METHODS BASED ON RANDOMLY SHIFTED LATTICE RULE FOR COMPUTATION OF MULTIPLE INTEGRALS

Venelin Todorov, Valentin Dimitro, Iliyn Tsvetkov.....21

### APPLICATION OF AUTODESK SOFTWARE PRODUCT FOR TRAINING OF STUDENTS IN GENERAL ENGINEERING

Anton Antonov.....31

## Geodesy

---

### DETERMINATION OF VISIBILITY BETWEEN CARD POINTS

Sabin Ivanov.....36

### DETERMINING THE SCALE OF A TOPOGRAPHIC MAP

Sabin Ivanov.....41

## Biology

---

### ESOPHAGEAL CARCINOMA AND BLOOD GROUP AFFILIATION

Velislav Todorov, Maria Boycheva, Volodia Georgiev, Cvetan Minkov, Milen Boichev, Rada Georgieva.....46

## Physics

---

### HEAT – MECHANICALLY INDUCED STRUCTURE DEVELOPMENT IN PARTIALLY CRYSTALLINE POLYESTER FIBERS. INFLUENCE OF THE MECHANICAL STRESS

Valentin Velev, Nina Arhangelova, Daniela Nedeva, Zhenya Stoyanova, Anton Popov.....52





---

## **MODELING AND ANALYSIS OF THE "AIRPLANE-AUTOPILOT" SYSTEM IN DESCENDING ATMOSPHERIC DISTURBANCE**

**P. Getsov\*\*\*, D. Jordanov\*\*, WangBo\*, St. Getsov\*\***

*\*NINGBO UNIVERSITY OF TECHNOLOGY-CHINA;*

*\*\*SPACE RESEARCH AND TECHNOLOGY INSTITUTE –BAS, BULGARIA*

*E-mail: bo305@hotmail.com, director@space.bas.bg,  
djordanov@space.bas.bg*

**ABSTRACT:** *The study examined the behavior of the "autopilot-airplane" system under a strong downward impulse. The airplane is modeled through a complex turbulent turbulence that forms at mountain peaks. The airplane's behavior is controlled and controlled by various autopilots. Comments and conclusions were made on the results of modeling for a possible catastrophic situation if the stock height is less than 50 m and the control is from a simple pilot structure.*

**KEY WORDS:** *FLIGHT SAFETY, MODELING, CONTROL CONTROL, FLIGHT DYNAMICS.*

### **Problem under investigation**

Passage of an area with severe atmospheric disturbance is always associated with potentially dangerous consequences for the airplane, crew and passengers. A case is considered a flight with an autopilot and the following questions are answered:

- When the autopilot can complicate the flight and create a crash hazard?
- Should the autopilot be switched off when flying in high atmospheric disturbance?

### **Study method**

As a far as flights in strong atmospheric disturbance are always considered to be one of the major versions for a number of crashes and accidents, flights in such areas are potentially dangerous, and the flight

instructions define the means for safe passage in automatic or manual control. Answers to questions put in the research can be solved by modeling and such a method is chosen for the specific situation.

### 1. Introduction

In flight practice, there is a view that autopilot should be excluded in conditions of strong turbulence and other atmospheric disturbances associated with upward or especially more dangerous downward gusts in restricted space areas. This issue is controversial, especially for modern aviation, and in most cases is related to the level of technology in the area of automatic control systems. There is no adequate response valid for all cases and the pilot should therefore follow the specific instructions. A common answer can be given by modeling a type situation where the consequences of the management of different autopilots have been checked.

### 2. Ways to solve the problem

In order to achieve the objectives set in the study, Matlab-Simulink was modeled on a hypothetical subsonic maneuver in automatic mode of flying over a mountain peak of about 2000 meters with a strong counter-wind, where before flit over a mountain peak and to the airplane hit downward gusts of about 17 m / s. A common pattern of the modeled flight is shown in Figure 1.

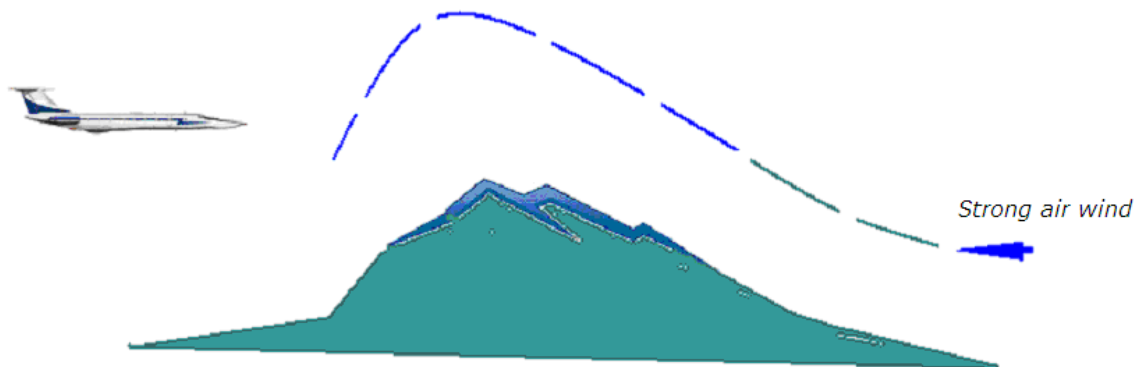


Fig.1. Scheme of the modeled situation

### 3. Solution of the research problem

The "autopilot" system has been tested for two types of autopilot. The first type has the simplest structure and law for elevator:

$$\delta_\epsilon = K_\epsilon^\vartheta (\vartheta - \vartheta_{\text{заданено}}) + K_\epsilon^{\omega_z} \omega_z ; \quad (1)$$

The second type of autopilot is with vertical speed signals and height control and stabilization.

$$\delta_\epsilon = K_\epsilon^H (H - H_{\text{заданено}}) + K_\epsilon^{V_y} V_y + K_\epsilon^\vartheta (\vartheta - \vartheta_{\text{заданено}}) + K_\epsilon^{\omega_z} \omega_z \quad (2)$$

The indices and designations in the control laws correspond to the modeling in GOST 20058-80 according to the longitudinal motion equations known from the flight dynamics (3) and have the following meanings:

- $\delta_\epsilon$  - Variation of the steering elevator (degrees);
- $K_\epsilon^H$  - Transmission coefficient for the flight height control channel;
- $K_\epsilon^{Vy}$  - Transmission coefficient of the channel at the vertical speed.
- $K_\epsilon^g$  - gearbox in the pitch pitch channel;
- $K_\epsilon^{\omega_z}$  - Transmission coefficient at tangent angular velocity;
- $g$  - pitch angle (degrees);
- $\omega_z$  - angular velocity of pitch (degrees / s);
- $H$  - flight height (m);
- $V_y$  - Vertical speed (m / s)

The general appearance of the model is shown in Fig.2

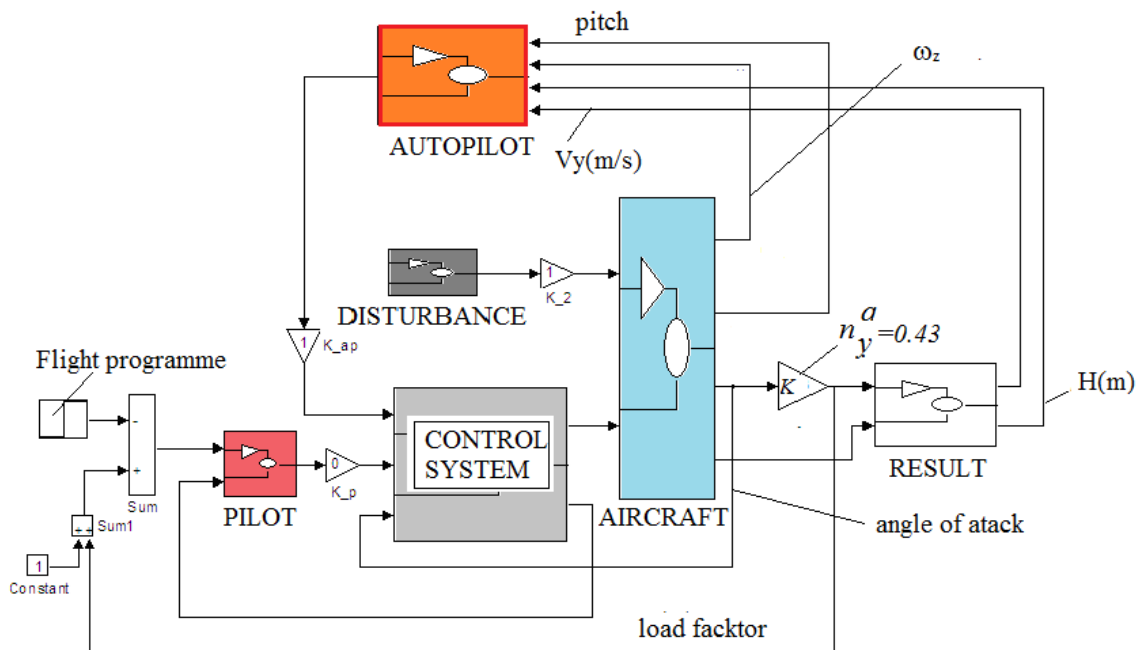


Fig.2. General appearance of the model

#### 4. Results

Figures 3 and 4 show results of the airplane response without autopilot control during a downward flight. The elevator is fixed around the mode balance.

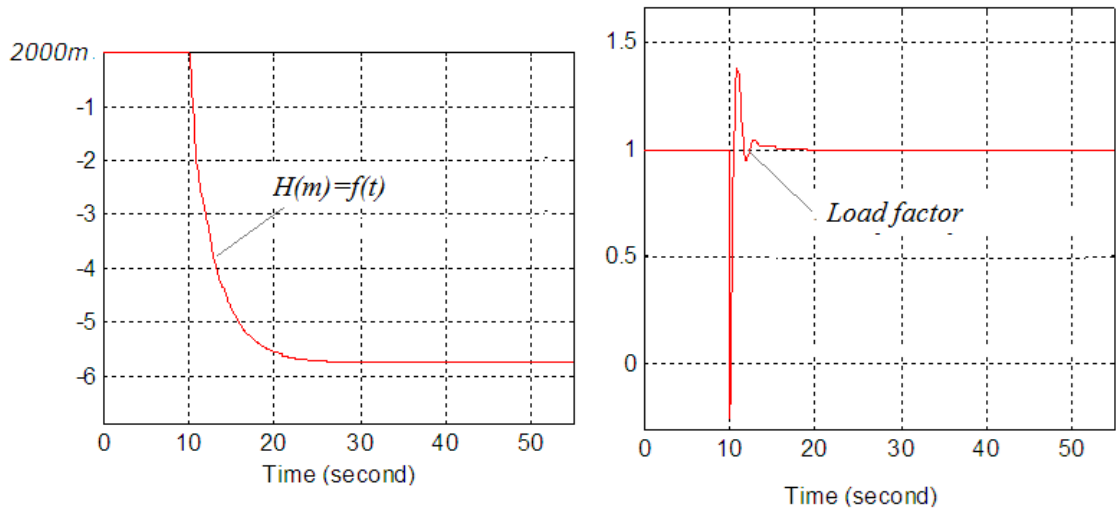


Fig. 3. Flight height change and normal overload without autopilot control.

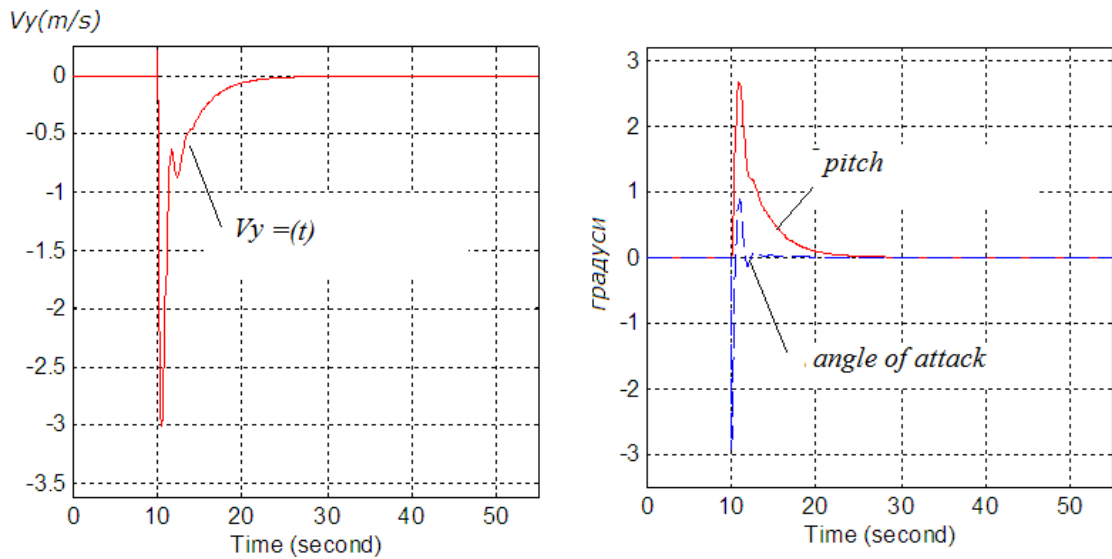


Fig.4. Modification of vertical speed, pitching angle and attack without autopilot control (only changes are added to the output mode)

Figures 5 and 6 show the reaction results of an autopilot control with a simplified control law structure (Law 1) when passing through a downward air storm.

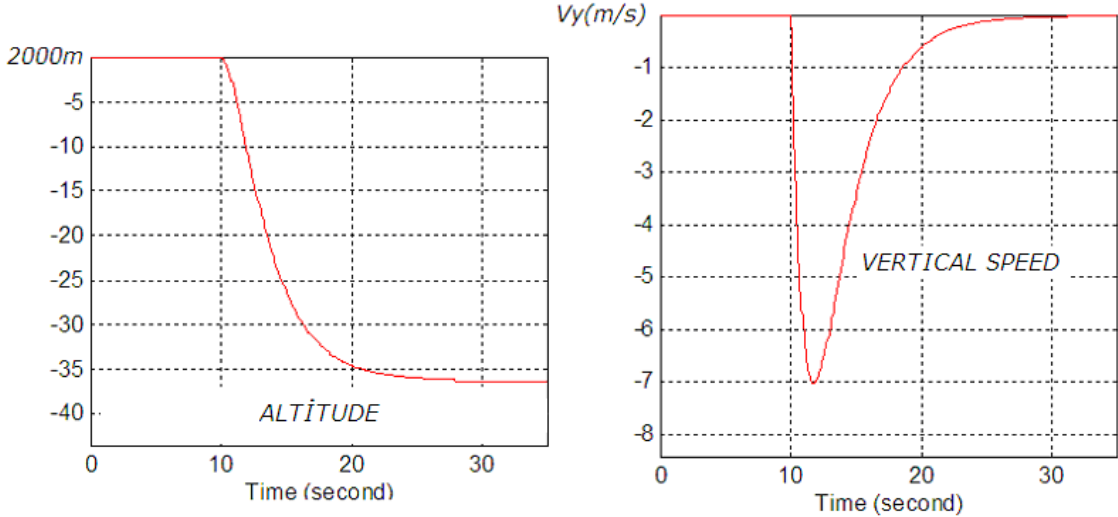


Fig.5. Flight altitude and vertical speed change from autopilot control with simplified control law structure - autopilot does not restore flight height

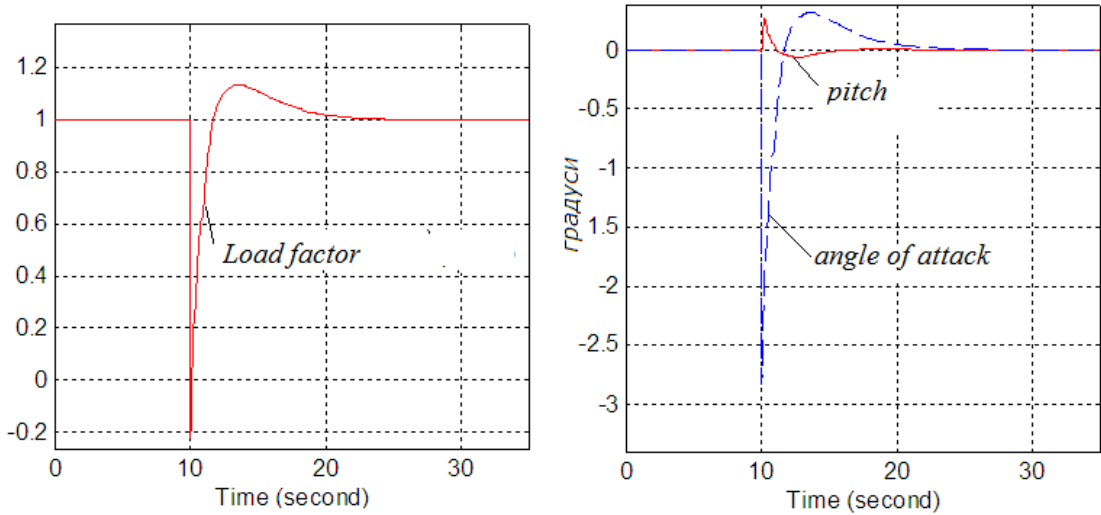


Fig.6. Modification of normal overload and pitch corners and autopilot control attack with simplified control law structure

Figures 7 and 8 show the reaction results of the autopilot control with law 2 (with altitude and vertical speed signals) when passing through the simulated atmospheric disturbance (downward air gust around a mountain peak).

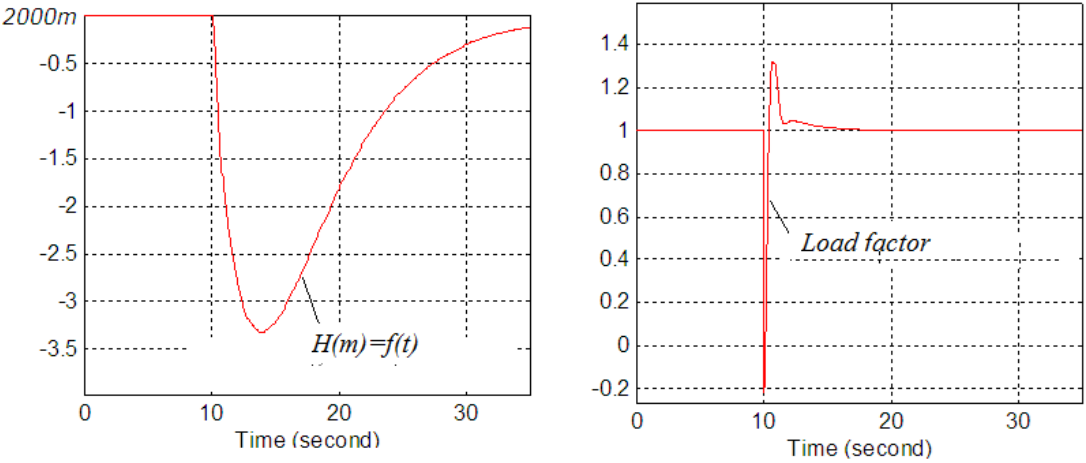


Fig.7. Flight height change and normal overload on autopilot control with altitude and vertical speed signals

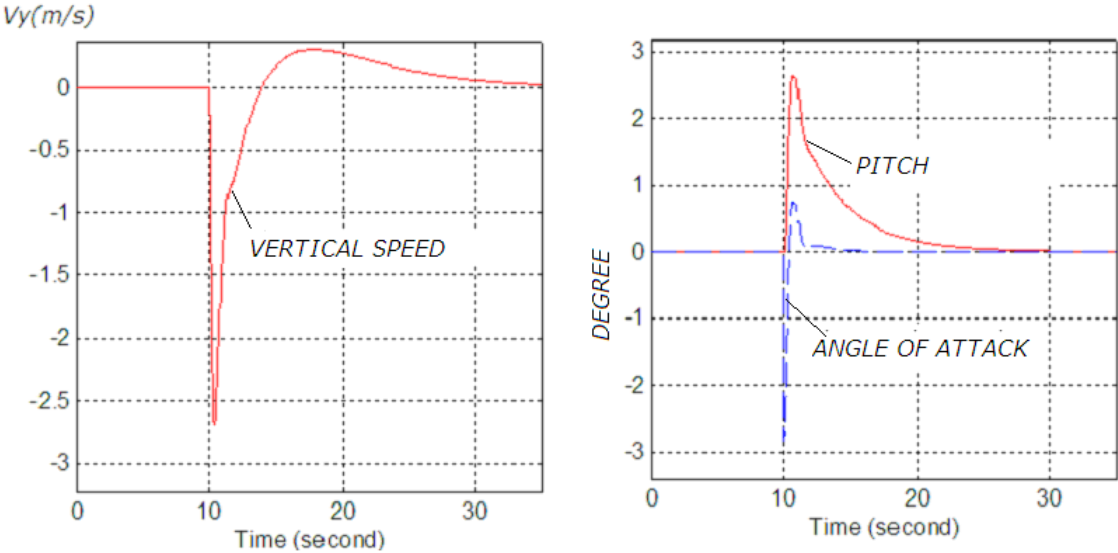


Fig.8. Modification of vertical speed, pitching angles and autopilot control with altitude and vertical speed signals

## 5. Conclusion of modeling and conclusions

- The modeling results (Figures 3 and 4) show that when overfly through a downward atmospheric impulse, the overload resistant airplane "go under", but it seeks to increase its pitch angle and thereby lessens the negative effects of gust. "Go under" in height is limited in this case to 5 to 6 meters, and the horizontal flight continues about 6 km with a lower altitude. This behavior is also referred to as "getting into an air pit". The pilot can not pilot exactly and is not advised to seek to limit the movement of the controls by increasing the pitch of the pitch because it will increase the collapse (the plane go under with the rear and the nose is lifted). Such behavior of the pilot is called "allowing the airplane to be entrapped in the disturbed atmosphere."
- In autopilot control with simplified structure (with tangent angle signals and angular velocity of pitching - results in Figures 5 and 6), the autopilot complicates the situation and the "dropping" is about 35 ... 40 meters at a high vertical speed (more from 7m / s). There is a real danger that the autopilot may cause a catastrophic situation to develop (in this case - falling on over a mountain peak or before it). If the airplane is equipped with such an autopilot, it should be switched off when passing through zones of any atmospheric disturbance.
- The autopilot with altitude and vertical speed signals quickly recovers flight altitude, fly down with a small vertical speed, and including such an autopilot when flying across some atmospheric disturbances is useful for flight safety. The modeling results are shown in Figures 7 and 8.
- The physiological impact on the pilot is almost the same for all modeled cases - in fast portions the normal overload reaches negative values and the pilot's body has a tendency to "hangs on the belts". The change in pitch and attack angles for the cases under consideration differs only by value but not by type - always at the beginning of the downward gust, the plane increases the angle of the pitch and reduces the angle of attack - ie. "Falling" has with the tail down.

### References:

- [1]. Mihalev IA, ВНОкоehov, IGGPavlina, MSChikulaev, NM.Eidinov Systems automated control aircraft - methods analysis and races ed. "Machine Building", Moscow 1971.
- [2]. Mihalev IA, ВН Окоehov, IG Pavlina, MS Shikulaev, Y.F. Киселев Системы автоматического и директорного управления авиатом изд. "Machine Building", Moscow 1974
- [3]. Galashev ES, NM Лысенко и др. Аэродинамика и динамика полета маневренных самолетов, ВИ, Москва 1984г.

- [4]. Гулѣтяев А.К. MATLAB 5.2 - Imitation Modeling in Windows Environment - Practical Instrument, St. Petersburg, ed. "Korona print" 1999
- [5]. 5.Jordanov D., Gecov P. "Unmanned aircraft – modeling and control", Third Scientific Conference with International Participaton, „SPACE, ECOLOGY, NANOTECHNOLOGY, SAFETY“, 27–29 June 2007, Varna, Bulgaria.
- [6]. Jordanov D., Gecov P., "CONTROL THROUGH MODEL OF UNMANNED AIRCRAFT", XV International Conference on Transport, Construction, Road and Lifting Transport Equipment and Technologies, 18-20.09. 2008 Sozopol, [http: /www.trans-MOTOAUTO.com](http://www.trans-MOTOAUTO.com)
- [7]. Jordanov D., S.Fotev "Autopilot Failures During Operation of the Unmanned Complex" International UNMANNED VEHICLES Workshop UVW 2010 10-12 June , Istanbul, Turkiye, [www.hho.edu.tr/uvw2010](http://www.hho.edu.tr/uvw2010).
- [8]. Yordanov D. Design and Research of the "Unmanned Airplane" -Autopilot System by Computer Analogue "SPACE, ECOLOGY, SAFETY" 2 - 4 November 2016, Sofia, Bulgaria, [http: /www.space.bas.bg](http://www.space.bas.bg)
- [9]. Yordanov D., Getsov S., "Investigation of the Role of the Flight Safety Management System" Twelfth Scientific Conference with International Participation "SPACE, ECOLOGY, SAFETY" 2 - 4 November 2016, Sofia, Bulgaria, <http://www.space.bas.bg>
- [10].10. P. Getsov ,Wang Bo, D. Zafirov,G. Sotirov,St. Nachev,R. Yanev,P. Gramatikov ,V. Atanassov,H. Lukarski,S. Zabunov,AN UNMANNEDAERIAL SURVEILLANCE SYSTEM IN URBAN ENVIRONMENTS,Aerospace Research in Bulgaria,2018,29,<http://www.space.bas.bg>

### **Acknowledgements**

I. The study was performed with the use of the base:

1. Set up under the project BG161PO003-1.2.04-0053 "Information complex for aerospace environmental monitoring" (IKAMOS), financed by the operational program "Development of the competitiveness of the Bulgarian economy "2007-2013, co-financed by the European regional development fund and from the national budget of the Republic of Bulgaria.

2. Project "Strengthening and Expansion of the Aerospace Technology Transfer Office in the Field of Protection of Citizens' Health in Disasters" - BG161PO003-1.2.02 under the Operational Program "Development of the Competitiveness of the Bulgarian Economy" 2007-2013"

II. The authors gratefully acknowledge the support of K. C. Wong Education Foundation.



## QUASI-MONTE CARLO METHODS FOR COMPUTATION OF MULTIDIMENSIONAL INTEGRALS RELATED TO BAYESIAN MODELS IN INTERNATIONAL MIGRATION FORECASTING

Venelin Todorov<sup>1,2</sup>, Valentin Dimitrov<sup>3</sup>, Iliyan Tsvetkov<sup>3</sup>, Yuri Dimitrov<sup>4</sup>

<sup>1</sup> INSTITUTE OF MATHEMATICS AND INFORMATICS, BULGARIAN ACADEMY OF SCIENCES, DEPARTMENT OF INFORMATION MODELING, ACAD. GEORGI BONCHEV STR., BLOCK 8, 1113 SOFIA, BULGARIA

<sup>2</sup> INSTITUTE OF INFORMATION AND COMMUNICATION TECHNOLOGIES, BULGARIAN ACADEMY OF SCIENCES, DEPARTMENT OF PARALLEL ALGORITHMS, ACAD. G. BONCHEV STR., BLOCK 25 A, 1113, SOFIA, BULGARIA

<sup>3</sup> ROUSSE UNIVERSITY "ANGEL KANCHEV"

<sup>4</sup> UNIVERSITY OF FORESTRY, SOFIA, DEPARTMENT OF MATHEMATICS AND PHYSICS

*E-mail: vtodorov@math.bas.bg, venelin@parallel.bas.bg*

**ABSTRACT:** *The paper addresses selected methodological aspects of international migration forecasting. The new methods based on the Bayesian statistics have been recently developed. A fundamental problem in Bayesian statistics is the accurate evaluation of multidimensional integrals. A comprehensive experimental study based on Faure and Hammersley low discrepancy sequences and Fibonacci based lattice rule has been done. The numerical tests show that the stochastic algorithms under consideration are efficient tool for computing multidimensional integrals. It is important in order to obtain a more accurate and reliable interpretation of the results in Bayesian statistics which is a foundation in international migration forecasting.*

**KEYWORDS:** *Quasi-Monte Carlo sequences, multidimensional integrals, Hammersley sequence, Fibonacci lattice rule, Faure sequence, international migration forecasting, Bayesian statistics.*

### Introduction

Forecasting international migration is an important, yet difficult research task, characterized by the highest errors among the forecasts of all components of the demographic change [1]. Reasons for this include a lack of a comprehensive migration theory, difficulties in the theoretical framework of

migration [5], uncertainty of potential explanatory variables, ignoring forced migration and policy elements in the forecasts, as well as poor data quality [3]. In order to improve accuracy of the international migration forecasts, attempts should be also made to improve the forecasting methodology [1,2,3].

### **Bayesian model for forecasting international migration**

The main drawback of a majority mathematical models of migration, apart from the event-history analysis, is that they themselves do not explicitly address the issue of uncertainty, important for preparing any forecast on their basis [3]. Although some of the models apply Markov chains [5,10,11], and can be therefore used to assess uncertainty using simulations, this possibility has not been explored up to date. However, the assessments of uncertainty may be also included in a majority of demographic models (cohort-component, multi-regional, or multi-state) by feeding them at input with stochastic forecasts of particular components of demographic change. The latter may involve econometric forecasts and time series models, both in the sample-theory and the Bayesian frameworks.

In the last few years an alternative approach based on the paradigm of Bayesian statistics has been developed in [3]. The methodology that would combine the advantages of the existing ones, including both the formality of the applied statistical tools, and including subjective expert judgment in the forecasting model is presented in [3]. This methodology allows for construction of forecasting models combining the formal methods with the subjective expertise [2,3].

Forecasting in the Bayesian approach is based on the construction of a probability distribution of the vector of future values of the variable under study, conditional on the vector of past (observed) values, and taking into account the posterior knowledge on the parameters of the forecasting model [7]. Bayesian methodology can reduce the estimation and prediction errors, in case the prior distribution is informative and consistent with the observations [3,4,9]. This is important in the small-sample studies (e.g., with population disaggregated by sex, age, regions, etc.), where the prior information has relatively more weight in the posterior result than the observations, unlike in large datasets [6,9]. The extreme estimates obtained from small-sample data are in this way corrected towards the prior expectations. The same applies to forecasting models based on short time series, where the Bayesian approach is a way to reduce uncertainty [23]. Additionally, the Bayesian methodology allows for a formal model selection in order to maximally utilize information from the sample, by comparing the posterior odds of different models given the data [22].

A fundamental problem in this methodology is the accurate evaluation of multidimensional integrals. High dimensional integrals are usually solved with

Monte Carlo algorithms. Monte Carlo method is the only possible method for high-dimensional problems since its convergence is independent of the dimension. Monte Carlo methods give statistical estimates for the functional of the solution by performing random sampling of a certain random variable whose mathematical expectation is the desired functional. Monte Carlo methods are methods of approximation of the solution to problems of computational mathematics, by using random processes for each such problem, with the parameters of the process equal to the solution of the problem. The method can guarantee that the error of Monte Carlo approximation is smaller than a given value with a certain probability [8].

### **Quasi-Monte Carlo algorithms for numerical integration**

In the last few years new approaches have been developed that outperform standard Monte Carlo in terms of numerical efficiency. It has been found that there can be efficiency gains in using deterministic sequences rather than the random sequences which are a feature of standard Monte Carlo. These deterministic sequences are carefully selected so that they are well dispersed throughout the region of integration. Sequences with this property are known as low discrepancy sequences. These sequences are often more efficient than standard Monte Carlo in evaluating high dimensional integrals if the integrand is sufficiently regular.

They are usually superior to the Monte Carlo methods as they have a convergence rate of  $((\log N)^s/N)$ , where  $N$  is the number of samples and  $s$  is the dimensionality of the problem under consideration.

The standard  $M$ -dimensional Hammersley sequence [13] based on a number of samples  $N$  is simply composed of a first component of successive fractions  $0/N, 1/N, \dots, N/N$ , paired with  $M-1$  1-dimensional van der Corput sequences [20], using as bases the first  $M-1$  primes. The van der Corput sequence generates a sequence of points in  $[0,1]$  which never repeats. For positive index  $I$ , the elements of the van der Corput sequence are strictly between 0 and 1. In particular, the  $I$ -th element of the van der Corput sequence is computed by writing  $I$  in the base  $B$  (usually 2) and then reflecting its digits about the decimal point. Let  $b_1, \dots, b_{s-1}$  be coprime positive integers greater than 1. For given  $s$  and  $N$ , the  $s$ -dimensional Hammersley set of size  $N$  is defined by [14]

$$x(n) = (g_{b_1}(n), \dots, g_{b_{s-1}}(n), \frac{n}{N})$$

for  $n = 1, \dots, N$ . Then the discrepancy of the set is obtained in [13]:

$$D_N^*(x(1), \dots, x(N)) \leq C \frac{(\log N)^{s-1}}{N}$$

where  $C$  is a constant depending only on  $b_1, \dots, b_{s-1}$ . The above estimation for the discrepancy of the Hammersley sequence means that this is a low

discrepancy sequence. The parameters of the algorithm are input: the integer  $I$ , the index of the element of the sequence  $0 \leq I$ ; integer  $M$ , the spatial dimension,  $1 \leq M \leq 100$  and integer  $N$ , the "base" for the first component  $1 \leq N$ . Output is real  $R(M)$ , the element of the sequence with index  $I$ .

The monographs of Sloan and Kachoyan [19] and Wang and Hickernell [21] provide comprehensive expositions of the theory of integration lattices.

Let  $n$  be an integer, and  $a = (a_1, \dots, a_s)$  be an integer vector modulo  $n$ . A set of the form [15]

$$P_n = \left\{ \left\{ \frac{ak}{n} \right\} = \left( \left\{ \frac{a_1 k}{n} \right\}, \dots, \left\{ \frac{a_s k}{n} \right\} \right) \mid k = 1, \dots, n \right\}$$

is called a lattice point set, where  $\{x\}$  denotes the fractional part of  $x$ . The vector  $a$  is called a lattice point or generator of the set. As one can see, the formula for the lattice point set is simple to program. The difficulty lies in finding a good value of  $a$ , such that the points in the set are evenly spread over the unit cube.

The choice of good

generating vector, which leads to small errors, is not trivial. We consider the following generating vector based on generalized Fibonacci numbers of corresponding dimensionality:

$$a = (1, F_{l+1}^{(s)}, \dots, F_{l+s-1}^{(s)}), \quad n_l = F_l^{(s)},$$

where

$$F_{l+s}^{(s)} = F_l^{(s)} + F_{l+1}^{(s)} + \dots + F_{l+s-1}^{(s)}, \quad l = 0, 1, \dots$$

with initial conditions

$$F_0^{(s)} = F_1^{(s)} = \dots = F_{s-2}^{(s)} = 0, \quad F_{s-1}^{(s)} = 1,$$

for  $l=0, 1, \dots$

The discrepancy of the set obtained by using the vector described above is asymptotically estimated in [21].

The number of calculation required to obtain the generating vector is  $O(\ln n_l)$ . The generation of a new point requires constant number of operations, thus to obtain a lattice set of the described kind consisting of  $n_l$  points,  $O(\ln n_l)$  number of operations are necessary.

The Faure sequences [13] are a digital  $(0, s)$ -sequence over  $\mathbf{F}_b$  with  $b$  denoting a prime (original case) or a prime power (general case) greater or equal to  $s$ . The  $s$  infinite generator matrices  $\mathbf{C}^{(1)}, \dots, \mathbf{C}^{(s)}$  over  $\mathbf{F}_b$  are defined by  $\mathbf{C}^{(i)} = (c_{jr}^{(i)})_{j,r \geq 0}$

$$\text{with } c_{jr}^{(i)} = \binom{r}{j} \alpha_i^{r-j},$$

where  $\alpha_1, \dots, \alpha_s$  denote  $s$  distinct elements from  $\mathbf{F}_b$  and the conventions  $\alpha^0 = 1$  for all  $\alpha \in \mathbf{F}_b$  and  $\binom{r}{j} = 0, j > r$ .

For  $\alpha = 1$ , the resulting matrix is the infinite Pascal matrix modulo the characteristic of  $\mathbf{F}_b$ ; for  $\alpha = 0$ , it is the infinite identity matrix. If  $s = 1$  and  $\alpha_1 = 0$ , the resulting  $(0, 1)$ -sequence is identical to the van der Corput sequence in the same base [20]. The algorithm for the Faure sequence follows the method of Henri Faure in [12] for computing quasi-random numbers. It is a merging and adaptation of the routines INFAUR and GOFAUR from ACM TOMS 647. We use of persistent variables to improve the MATLAB implementation. The parameters of the Faure algorithm are described below. The input is an integer DIM\_NUM, the spatial dimension, which should be at least 2. The other parameter is integer SEED, which is the seed, that indicates the index of the element of the sequence to be calculated. If SEED is negative, it is effectively replaced by a more suitable value. The output is a real QUASI(DIM\_NUM), the next quasi-random vector. For the output the appropriate value of SEED have to be used on the next call, if the next element of the sequence is desired [4].

### Numerical example and results

We will be interested in the following integrals that have widely used in Bayesian statistics:

$$\int_{\Omega} e^{-Nf(x)} \phi(x) dx,$$

where  $f(x)$  and  $\phi(x)$  are  $s$ -dimensional polynomials and  $N$  is a natural number. This integrals are investigated by Shaowei Lin in [14]. We will test the performance of the Faure sequence (FAUR), the Hammersley sequence (HAM) and a particular lattice rule with generating vector, based on the generalized Fibonacci numbers of the corresponding dimensionality (FIBO). We will consider the following 7 and 15 dimensional integrals (Example 1 and Example 2 respectively):

$$\int_{[0,1]^7} e^{1 - \sum_{i=1}^3 \sin(\frac{\pi}{2} \cdot x_i)} \cdot \arcsin \left( \sin(1) + \frac{\sum_{j=1}^7 x_j}{200} \right) \approx 0.7515.$$

$$\int_{[0,1]^{15}} \exp \left( - \prod_{i=1}^{15} x_i \right) dx \approx 0.999.$$

Table 1: The relative error for 7 dimensional integral

N	FAUR	FIBO	HAM
100	9.81e-2	9.26e-2	1.64e-1
1000	1.03e-3	2.21e-2	6.59e-2
10000	3.34e-4	1.59e-3	6.45e-2
100000	3.40e-4	9.14e-5	8.17e-3

Table 2: The computational time for 7 dimensional integral

time in seconds	FAUR	FIBO	HAM
0.1	8.17e-2	2.17e-2	3.19e-1
1	2.26e-3	9.32e-3	8.12e-2
10	2.34e-4	2.47e-3	6.45e-2
60	1.10e-4	1.15e-4	8.69e-3

Table 3: The relative error for 15 dimensional integral

N	FAUR	FIBO	HAM
100	7.45e-3	3.04e-5	6.44e-4
1000	7.86e-4	3.04e-5	1.95e-4
10000	1.26e-4	1.23e-5	7.27e-5
100000	6.43e-5	7.99e-6	7.51e-5

Table 4: The computational time for 15 dimensional integral

time in seconds	FAUR	FIBO	HAM
0.1	5.56e-3	1.22e-4	5.94e-2
1	6.58e-4	7.80e-5	1.24e-3
10	1.06e-4	7.60e-5	9.46e-4
60	7.17e-5	1.38e-5	6.65e-5

In the Table 1 and 2 are presented the relative error for the 7 and 15 dimensional integrals with Fibonacci lattice sequence (FIBO), Faure low discrepancy sequence (FAUR) and Hammersley quasi-random sequence (HAM) for a fixed number of points. In Table 2 and 4 are presented the relative errors for 7 and 15 dimensional integrals with FAUR, FIBO and HAM for a fixed computational time which is a measure of the computational complexity. Obviously FIBO has the lowest computational complexity and is the fastest algorithm, while HAM and FAUR are slower, because they need an additional time for generating the corresponding low discrepancy sequences. As can be seen from the results for 7 dimensional integral, the low discrepancy sequence of Hammersley produces the worst results. It is interesting to see that Faure

sequence gives lowest relative errors for a given number of realizations of the random variable - see Table 1, but the Fibonacci lattice sequence has the advantage for a preliminary given time in seconds - see Table 2. For 15 dimensional integral Fibonacci gives the best results for a given number of realizations and fixed computational time - see Table 3, while Hammersley sequence and Faure sequence have very similar behavior - see Table 4. So we can conclude that all stochastic algorithms under consideration are efficient tool for evaluation of multidimensional integrals related to Bayesian models in migration forecasting. This is the first time a particular 1-rank lattice rule based on Fibonacci generating vector is compared with Hammersley and Faure quasi-random sequences.

### **Conclusion**

In this paper we analyze the performance of different quasi-Monte Carlo methods for multidimensional integrals related to Bayesian based models in improving the international migration. Stochastic methods under consideration are an efficient way to solve problems in forecasting international migration based on Bayesian statistics. A fundamental problem in Bayesian statistics is the accurate evaluation of the presented multidimensional integrals. It is a crucial element since this may be important for improving the international migration forecasting.

### **Acknowledgement**

The author Venelin Todorov is supported by the Bulgarian Academy of Sciences through the „Program for Career Development of Young Scientists", Grant DFNP-17-88/28.07.2017, Project „Efficient Numerical Methods with an Improved Rate of Convergence for Applied Computational Problems", by the Bulgarian National Fund of Science under Project DN 12/5-2017, "Efficient Stochastic Methods and Algorithms for Large-Scale Problems", by the Bulgarian National Fund of Science under Project DN 12/4-2017, "Advanced Analytical and Numerical Methods for Nonlinear Differential Equations with Applications in Finance and Environmental Pollution".

### **References**

- [1]. J. Alho, (1990). Stochastic methods in population forecasting. *International Journal of Forecasting*, 6 (4), 521–530.
- [2]. M.J. Bayarri, and J. O. Berger (2004). The Interplay of Bayesian and Frequentist Analysis. *Statistical Science*, 19 (1), 58–80.
- [3]. Jakub Bijak, Bayesian methods in international migration forecasting, 2008, In book *International migration in Europe: Data, Models and Estimates*, Chapter 12, <https://onlinelibrary.wiley.com/doi/abs/10.1002/9780470985557.ch12>
- [4]. Paul Bratley, Bennett Fox, Harald Niederreiter, *Implementation and Tests of*

Low Discrepancy Sequences, ACM Transactions on Modeling and Computer Simulation, Volume 2, Number 3, July 1992, pages 195-213.

- [5]. L.A. Brown, (1970). On the use of Markov chains in movement research. *Economic Geography*, 46 (Suppl.), 393–403.
- [6]. H. Brücker and B. Siliverstovs (2005). *On the Estimation and Forecasting of International Migration: How Relevant is Heterogeneity Across Countries*. IZA Discussion Paper 170. Bonn: Institut zur Zukunft der Arbeit.
- [7]. P. Congdon, 2003, *Applied Bayesian Modelling*. Chichester: John Wiley.
- [8]. I. Dimov, Monte Carlo Methods for Applied Scientists, New Jersey, London, Singapore, World Scientific, 2008, 291p.
- [9]. Dzhurov V. Application of Summarized Functions for Information Source Protection, Journal Scientific and Applied Research, 2013, No 3, pp. 51-56.
- [10]. Dzhurov V., Kostova M., Dzhurov K. Application of Probability Neural Networks for Classification of Explosives with Blasting Action. Mathematics in Industry, Cambridge Scholars Publishing, 2014, 254-285.
- [11]. Dzhurov V., Slavova A., Kostova M., Tsakoumis A., Mladenov V.. Processing of Radiographic Image with CNN Neural Network. WSEAS Transactions on Signal Processing, 2005, No 1, pp. 67-72.
- [12]. Henri Faure, Discrepance de suites associees a un systeme de numeration (en dimension s), Acta Arithmetica, Vol. 41, 1982, 337-351.
- [13]. John Hammersley, Monte Carlo methods for solving multivariable problems, Proceedings of the New York Academy of Science, Volume 86, 1960, 844-874.
- [14]. J.M. Hammersley, D.C. Handscomb, (1964). Monte Carlo Methods.
- [15]. L.K. Hua, Y. Wang: Applications of Number Theory to Numerical analysis, 1981.
- [16]. J.A. Hoeting, D. Madigan, A. E. Raftery, and C. T. Volinsky (1999). Bayesian Model Averaging: A Tutorial. *Statistical Science*, 14 (4), 382–417.
- [17]. Lin S., “Algebraic Methods for Evaluating Integrals in Bayesian Statistics,” UC Berkeley, May 2011.
- [18]. Rogers, A. (1966). A Markovian Policy Model of Interregional Migration. *Papers of the Regional Science Assoc.*, 17, 205–224.
- [19]. I.H. Sloan and P.J. Kachoyan, Lattice methods for multiple integration: Theory, error analysis and examples, (1987), J. Numer. Anal., 24, 116-128.
- [20]. Van der Corput, J.G.: Verteilungsfunktionen I-VIII. Proc. Akad. Amsterdam, Vol. 38 (1935) 813-821, 1058-1066, Vol.39 (1936) 10-19, 19-26, 149-153, 339-344.
- [21]. Y. Wang and F.J. Hickernell, An historical overview of lattice point sets, (2002).
- [22]. W. Weidlich and G. Haag (eds.) (1988). *Interregional migration: dynamic theory and comparative analysis*. Berlin-Heidelberg: Springer
- [23]. A. Zellner, (1971). *An Introduction to Bayesian Inference in Econometrics*. NY: John Wiley.



## A NUMERICAL STUDY ON QUASI MONTE CARLO METHODS BASED ON RANDOMLY SHIFTED LATTICE RULE FOR COMPUTATION OF MULTIPLE INTEGRALS

Venelin Todorov<sup>1,2</sup>, Valentin Dimitro, Iliyn Tsvetkov

<sup>1</sup> DEPARTMENT OF INFORMATION MODELING, INSTITUTE OF MATHEMATICS AND  
INFORMATICS, BULGARIAN ACADEMY OF SCIENCES

<sup>2</sup> DEPARTMENT OF PARALLEL ALGORITHMS, INSTITUTE OF INFORMATION AND  
COMMUNICATION TECHNOLOGIES, BULGARIAN ACADEMY OF SCIENCES

<sup>3</sup> ROUSSE UNIVERSITY "ANGEL KANCHEV"

*E-mail: vtodorov@math.bas.bg, venelin@parallel.bas.bg dvd@gmail.com,  
iliyan\_ts@yahoo.com;*

**ABSTRACT:** *A comprehensive numerical study between randomly shifted lattice rules and Fibonacci based lattice rule for computing multidimensional integrals has been done. The methods have not been compared before and both are recommended in case of smooth integrands. The two stochastic methods are completely different thus it is not trivial of which one of them outperforms the other. We consider a case study with smooth integrand functions of different dimensions.*

**KEYWORDS:** *Quasi-Monte Carlo sequences, multidimensional integrals, randomly shifted lattice rules, Fibonacci lattice rule*

### Introduction

Nowadays Monte Carlo (MC) and quasi-Monte Carlo (QMC) methods have become a popular computational device for many problems. Multidimensional integrals are usually solved with MC and QMC algorithms [11]. New approaches have been developed that outperform standard MC algorithm in terms of numerical efficiency [1]. It has been found that there can be efficiency gains in using deterministic sequences rather than the random sequences which are a feature of standard Monte Carlo [5]. The crude Monte Carlo method has rate of convergence  $O(N^{-1/2})$  which is independent of

the dimension of the integral, and that is why Monte Carlo integration is the only practical method for many high-dimensional problems [2]. Much of the efforts to improve MC methods are in construction of variance reduction methods which speed up the computation or to use quasi-random sequences [4]. QMC methods use deterministic sequences that have better uniform properties measured by discrepancy [12]. They are usually superior to the MC methods as they have a convergence rate of  $((\log N)^s/N)$ , where  $N$  is the number of samples and  $s$  is the dimensionality of the problem under consideration.

### Basic Definitions

Let  $G_s$  denote the unit cube in  $s$ -dimensional space [23]:

$$G_s = [0, 1]^s = \{x = (x_1, \dots, x_s) \mid 0 \leq x_j < 1, j = 1, \dots, s\}.$$

Let  $n_1 < n_2 < \dots$  be a sequence of positive integers, and let  $P_{n_l}$  be any set of  $n_l$  points in  $G_s$ . (Here a set may have multiple copies of the same point.) For any  $r = (r_1, \dots, r_s)$  note that  $r_1 \dots r_s$  is the volume of the box  $[0; r)$ . Let  $N_{n_l}(r)$  denote the number of points in  $P_{n_l}$  lying inside the box  $[0; r)$ . The discrepancy of the set  $P_{n_l}$  is defined as the largest difference between the proportion of points in the box and the volume of the box:

$$D(n_l) := \sup_{r \in G_s} \left| \frac{N_{n_l}(r)}{n_l} - r_1 \dots r_s \right|$$

This notion was introduced by Weyl (1916). If  $D(n_l) = o(1)$  as  $n_l$  goes to infinity, then the sequence of sets  $P_{n_l}$ ,  $n_1 < n_2 < \dots$  is said to be uniformly distributed on  $G_s$  with discrepancy  $D(n_l)$ . The subscript  $l$  is often omitted for simplicity. Not only is the discrepancy a geometric method for measuring uniformity of a set, the discrepancy of a set measures its quality for use in numerical quadrature. The error of this approximation is bounded by the Koksma-Hlawka inequality [14]:

$$\left| \int_{G_s} f(x) dx - \frac{1}{n} \sum_{k=1}^n f(x_k) \right| \leq D(n) \cdot V(f),$$

where  $D(n)$  is the discrepancy of the set

$$P(n) = \{x_1, \dots, x_n\},$$

and  $V(f)$  is the bounded variation of  $f$  in the sense of Hardy and Krause. If the integrand is smoother and also periodic, then better error bounds may be obtained, in particular for quadrature rules using lattice point sets.

The lattice  $S$  is an infinite set of points with the following three properties [16,17]:

1. If  $x$  and  $x'$  belong to  $S$ , then  $x + x'$  and  $x - x'$  also belongs to  $S$ .
  2.  $S$  contains  $s$  linearly independent points.
  3. There exists a sphere centered at 0 that contains only 0 itself.
- By a "lattice rule" then, we shall mean a rule of the form

$$I_N(f) = \frac{1}{N} \sum_{j=0}^{N-1} f(x_j),$$

in which  $x_0, \dots, x_{N-1}$  are all the points of a multiple-integration lattice that lie in  $G_s$ . The cubic lattice is

$$\left\{ \left( \frac{j_1}{n}, \dots, \frac{j_s}{n} : j_i \in \mathbb{Z}, 1 \leq i \leq s \right) \right\},$$

where  $n$  is a positive integer. The corresponding lattice rule is the "rectangle rule"

$$I_N(f) = \frac{1}{N} \sum_{j_1=0}^{n-1} \dots \sum_{j_s=0}^{n-1} f\left(\frac{j_1}{n}, \dots, \frac{j_s}{n}\right),$$

where  $N = n^s$ . Because  $N$  rises very rapidly with  $s$ , the rectangle rule suffers in a very obvious way from the "curse of dimensionality." Note that this rule is equivalent, because of the assumed periodicity, to a product-trapezoidal rule.

Lattice rules are based on the use of deterministic sequences rather than random sequences. They are a special type of so-called low discrepancy sequences. It is known that as long as the integrand is sufficiently regular, lattice rules outperform the basic Monte Carlo method and most of the other types of low discrepancy sequences [8,12].

### **Fibonacci based lattice rule for numerical integration**

There are constructions of sequences known such that for their discrepancy:

$$D_N^*(x_1, \dots, x_N) \leq C \frac{(\ln N)^s}{N}.$$

Here  $C$  is a certain constant, depending on the sequence. These sequences are believed to have the best possible order of convergence.

The monographs of Sloan and Kachoyan [18], Niederreiter [15], Hua and Wang [9], Wang and Hickernell [23] and Sloan and Joe [17] provide comprehensive expositions of the theory of integration lattices.

Let  $n$  be an integer, and  $a = (a_1, \dots, a_s)$  be an integer vector modulo  $n$ . A set of the form [19]

$$P_n = \left\{ \left\{ \frac{ak}{n} \right\} = \left( \left\{ \frac{a_1 k}{n} \right\}, \dots, \left\{ \frac{a_s k}{n} \right\} \right) \mid k = 1, \dots, n \right\}$$

is called a lattice point set, where  $\{x\}$  denotes the fractional part of  $x$ . The vector  $a$  is called a lattice point or generator of the set. As one can see, the formula for the lattice point set is simple to program. The difficulty lies in finding a good value of  $a$ , such that the points in the set are evenly spread over the unit cube. The choice of good

generating vector, which leads to small errors, is not trivial [9,10]. Complicated methods from theory of numbers are widely used, for example Zaremba's index or error of the worst function. We consider the following generating vector based on generalized Fibonacci numbers of corresponding dimensionality [9,23]:

$$a = (1, F_{l+1}^{(s)}, \dots, F_{l+s-1}^{(s)}), \quad n_l = F_l^{(s)},$$

where

$$F_{l+s}^{(s)} = F_l^{(s)} + F_{l+1}^{(s)} + \dots + F_{l+s-1}^{(s)}, \quad l = 0, 1, \dots$$

with initial conditions

$$F_0^{(s)} = F_1^{(s)} = \dots = F_{s-2}^{(s)} = 0, \quad F_{s-1}^{(s)} = 1,$$

for  $l=0,1,\dots$

The discrepancy of the set obtained by using the vector described above is asymptotically estimated in [9].

The number of calculation required to obtain the generating vector is  $O(\ln n_l)$ . The generation of a new point requires constant number of operations, thus to obtain a lattice set of the described kind consisting of  $n_l$  points,  $O(\ln n_l)$  number of operations are necessary. However the discrepancies of the lattice point sets obtained by these two methods have larger upper bounds than those obtained by Korobov's method [17,18].

### **Randomly shifted lattice rules**

The method is developed by Dirk Nuyens in [12,13]. Given a generating vector  $\mathbf{z}$  of integers, the  $k$ -th point of the sequence is given by

$$\mathbf{x}_k := \varphi(k) \mathbf{z} \bmod 1, \quad \text{for } k=0,1,2,\dots,$$

where  $\varphi$  is typically the radical inverse or the gray coded radical inverse function in the base of the lattice sequence. The radical inverse of an integer  $k$  with  $m$  digit base  $b$  expansion

$$k = (k_{m-1} k_{m-2} \dots k_0)_b$$

is obtained by mirroring the digits at the fractional point, i.e.,

$$\varphi(k) = (0.k_0 k_1 \dots k_{m-1})_b .$$

Obviously the result is a rational in  $b^m$  and an alternative view is thus to look at this mapping as a permutation of the integers in  $\{0, \dots, b^m - 1\}$ . In other words we are reversing the digits. Luckily, in base 2 reversing digits can be done efficiently. There is a Matlab/Octave and a C++ version to reverse bits developed by Dirk Nuyens in [13]. To obtain the radical inverse in base 2 of an unsigned 32 bit integer then just requires scaling the result of the bit reversion by  $2^{-32}$ .

Working in gray code ordering has speed advantages for digital nets (and sequences) but less so for lattice sequences. The comparison with the digital sequences will be a future study.

## Sobol Sequences

Sobol sequences (also called  $LP_\tau$  sequences or  $(t, s)$  sequences in base 2) are an example of quasi-random low discrepancy sequences. The Sobol quasi-random sequences was first introduced by the Russian mathematician Ilya M. Sobol in 1967 [19] and later described in [20]. We use an adaptation of the INSOBL and GOSOBL routines in ACM TOMS Algorithm 647 [4] and ACM TOMS Algorithm 659 [3]. The original code can only compute the "next" element of the sequence. The revised code allows the user to specify the index of the desired element [21]. These sequences use a base of two to form successively finer uniform partitions of the unit interval and then reorder the coordinates in each dimension. In his article, Sobol described  $\Pi_\tau$ -meshes and  $LP_\tau$  sequences, which are  $(t, m, s)$ -nets and  $(t, s)$ -sequences in base 2 respectively. The terms  $(t, m, s)$ -nets and  $(t, s)$ -sequences in base  $b$  (also called Niederreiter sequences) were coined in 1988 by Niederreiter [15]. The term Sobol sequences was introduced in late English-speaking papers in comparison with Halton, Faure and other low-discrepancy sequences. A more efficient gray code was proposed by Antonov and Saleev in [16].

## Numerical example and results

We will test the performance of the randomly shifted lattice rule (RSLR) based on a special choice of the generating vector obtained with the fast component by component construction developed by Dirk Nuyens [12,13] and a particular lattice rule with generating vector, based on the generalized Fibonacci numbers of the corresponding dimensionality (FIBO) on multidimensional integrals of smooth functions of different dimensions. A comparison with Sobol quasi-random sequence (SOBOL) for a preliminary given computational time will be given. We will be interested which of the methods gives lowest relative errors for 1 minute. We consider examples of 4, 10 and 25 dimensional integrals of smooth integrands. The computational time is given in seconds. We have used CPU Intel i5 2410M and 8GB of ram for running the numerical experiments and the computations have been done with Matlab.

Example 1.

$$\int_{[0,1]^4} x_1 x_2^2 e^{x_1 x_2} \sin(x_3) \cos(x_4) \approx 0.1089748630.$$

Exampe 2.

$$\int_{[0,1]^{10}} \frac{4x_1 x_3^2 e^{2x_1 x_3}}{(1+x_2+x_4)^2} e^{x_5+\dots+x_{10}} \approx 14.808435.$$

Example 3.

$$\int_{[0,1]^{25}} \frac{4x_1 x_3^2 e^{2x_1 x_3}}{(1+x_2+x_4)^2} e^{x_5+\dots+x_{20}} x_{21} \dots x_{25} \approx 103.808.$$

Table 1: The relative error for 4 dimensional integral

N	FIBO	Time	RSLR	Time
100	1.39e-1	0.001	1.31e-1	0.002
1000	9.27e-3	0.01	3.83e-3	0.02
10000	7.90e-4	0.09	5.76e-3	0.22
100000	3.40e-4	1.10	4.29e-4	2.24
1000000	2.68e-5	5.79	1.38e-5	16.5

Table 2: The computational time for 4 dimensional integral

time in seconds	FIBO	SOBOL	RSLR
0.1	9.27e-3	5.17e-3	3.44e-3
1	3.26e-4	5.37e-5	7.21e-4
10	7.21e-6	1.43e-5	9.21e-5
60	9.10e-8	2.68e-7	5.51e-6

Table 3: The relative error for 10 dimensional integral

N	FIBO	Time	RSLR	Time
100	8.35e-1	0.001	5.77e-1	0.002
1000	1.47e-1	0.08	6.72e-2	0.02
10000	4.21e-2	0.12	8.71e-3	0.25
100000	1.02e-2	0.91	9.57e-4	2.37
1000000	1.08e-3	6.27	1.95e-4	14.01

Table 4: The computational time for 10 dimensional integral

time in seconds	FIBO	SOBOL	RSLR
0.1	9.82e-2	1.06e-2	5.94e-2
1	4.58e-2	9.15e-2	8.12e-3
10	1.37e-2	9.93e-4	3.16e-4
60	1.28e-3	1.38e-4	1.65e-5

Table 5: The relative error for 25 dimensional integral

N	FIBO	Time	RSLR	Time
1000	9.84e-1	0.03	2.77e-1	0.04
10000	7.10e-1	0.11	9.70e-2	0.31
100000	1.97e-1	0.81	1.42e-3	2.59
1000000	9.09e-2	6.40	7.04e-4	11.1

Table 6: The computational time for 25 dimensional integral

time in seconds	FIBO	SOBOL	RSLR
0.1	7.10e-1	2.50e-1	4.22e-1
1	1.21e-1	1.09e-1	1.13e-1
10	8.86e-2	1.85e-2	4.43e-3
60	7.13e-2	9.21e-3	1.15e-4

In the Table 1,3 and 5 are presented the relative error for the 4,10 and 25 dimensional integrals with Fibonacci lattice sequence (FIBO) and randomly shifted lattice rule (RSLR) for a fixed number of points. In Table 2,4,6 are presented the relative errors for 4,10 and 25 dimensional integrals with Sobol quasi-random sequence (SOBOL), FIBO and RSLR for a fixed computational time which is a measure of the computational complexity. Obviously FIBO has the lowest computational complexity and is the fastest algorithm, while RSLR and SOBOL are slower, because they need an additional time for generating the corresponding low discrepancy sequences. As can be seen from the results for 4 dimensional integral, the randomly shifted lattice rule produces more rapid convergence, and lower errors, than the Fibonacci lattice sequence for a given number of realizations of the random variable-see Table 1, but for a fixed computational time- Fibonacci sequence gives better results- see Table 2. It can be seen that for lower dimensions FIBO is better than Sobol for a fixed computational time. Therefore Fibonacci lattice rule is the best choice for low dimensional integrals. For the 10-dimensional integral RSLR gives lower relative errors than the Fibonacci algorithm- see Table 3. For a preliminary given time in seconds Sobol and RSLR gives better results than Fibonacci-see Table 4. We can conclude that for mid and high dimensions RSLR sequence gives more reliable results than FIBO and it can be successfully compete with one of the best quasi-random sequences of Sobol. For 25- dimensional integral as expected FIBO produces the worst results, while randomly shifted lattice rule is more appropriate is clearly better - see Table 5. For a fixed computational time RSLR again gives lower relative errors than - see Table 6. For higher dimensions the errors can not be small. However, RSLR gives sufficient accuracy. This multidimensional integral can be applied to various problems [2] where data is taken in randomized way [6]. They are often used in physical problems [7] and are most useful when it is difficult or impossible to use other mathematical methods. This multidimensional integral can be applied to various problems like stochastic tomography connected with people migration. International migration is a topic that is attracting a significant level of interest in current political debate and is high on the agenda for policy makers in central and local government. In our previous paper [22] we described the Hammersley sequence and the comparison with the randomly shifted lattice rule and other types of low discrepancy sequences will be an object of a future study.

## **Conclusion**

In this paper we analyze the performance of different quasi-Monte Carlo methods for multidimensional integrals. Stochastic methods under consideration are an efficient way to solve the problem under consideration. Clearly the progress in this area is closely connected with developing fast and reliable algorithm for multidimensional integrals.

## Acknowledgement

This work was supported by the Bulgarian Academy of Sciences through the, Program for Career Development of Young Scientists", Grant DFNP-17-88/28.07.2017, Project „Efficient Numerical Methods with an Improved Rate of Convergence for Applied Computational Problems" and by the Bulgarian National Science Fund under Project DN 12/5-2017, Project “Efficient Stochastic Methods and Algorithms for Large-Scale Problems”.

## References

- [1]. N. Bakhvalov, On the approximate calculation of multiple integrals, Journal of Complexity, Volume 31, Issue 4, 2015, pp 502-516.
- [2]. P. Boyle, Y. Lai, K. Tan, (2001) Using Lattice Rules to Value Low-Dimensional Derivative Contracts.
- [3]. Paul Bratley, Bennett Fox, Algorithm 659: Implementing Sobol's Quasirandom Sequence Generator, ACM Transactions on Mathematical Software, Volume 14, Number 1, March 1988, pages 88-100.
- [4]. Paul Bratley, Bennett Fox, Harald Niederreiter, Implementation and Tests of Low Discrepancy Sequences, ACM Transactions on Modeling and Computer Simulation, Volume 2, Number 3, July 1992, pages 195-213.
- [5]. I. Dimov, Monte Carlo Methods for Applied Scientists, New Jersey, London, Singapore, World Scientific, 2008, 291p.
- [6]. Dzurov V. APPLICATION OF SUMMARIZED FUNCTIONS FOR INFORMATION SOURCE PROTECTION.// Journal Scientific and Applied Research, 2013, No 3, pp. 51-56, ISSN 1314-6289.
- [7]. Dzurov V, M.Kostova. I.Georgiev. A MATHEMATICAL MODEL SYSTEM FOR RADIOLOCATIONAL IMAGE RECONSTRUCTION OF DYNAMIC OBJECT WITH LOW RADIOLOCATIONAL VISIBILITY.// Proceedings of the Union of Scientists – Ruse, “Mathematics, Informatics and Physics”, 2012, No 9, pp. 35-40, ISSN 1314-3077.
- [8]. Hickernell, F. J., Hong, H. S., L'Ecuyer, P. and Lemieux, C. (2001), Extensible lattice sequences for quasi-Monte Carlo quadrature, SIAM J. Sci. Comput. 22, 1117-1138.
- [9]. Hua, L.K., Wang, Y.: Applications of Number Theory to Numerical analysis, 1981
- [10]. Ladislav Kocis, William Whiten, Computational Investigations of Low-Discrepancy Sequences, ACM Transactions on Mathematical Software, Volume 23, Number 2, 1997, pages 266-294.

- [11]. Kroese, D.P., Taimre, T., Botev, Z.: Handbook of Monte Carlo Methods, Wiley Series in Probability and Statistics, (2011)
- [12]. F.Y. Kuo and D. Nuyens, Application of quasi-Monte Carlo methods to elliptic PDEs with random diffusion coefficients - a survey of analysis and implementation, Foundations of Computational Mathematics, 16(6):1631-1696, 2016.
- [13]. Dirk Nuyens, The “Magic Point Shop” of QMC point generators and generating vectors,
- [14]. <https://people.cs.kuleuven.be/~dirk.nuyens/qmc-generators/> A. Owen: Monte Carlo theory, methods and examples, (2013)
- [15]. H. Niederreiter, Random Number Generation and quasi-Monte Carlo Methods, SIAM, 1992, ISBN13: 978-0-898712-95-7, LC: QA298.N54.
- [16]. V. M. Saleev, I. A. Antonov An Economic Method of Computing LP Tau-Sequences, USSR Computational Mathematics and Mathematical Physics, Volume 19, 1980, pages 252-256.
- [17]. I.H. Sloan and S. Joe: Lattice Methods for Multiple Integration, Oxford Uni Press, Oxford, 1994.
- [18]. I.H. Sloan and P.J. Kachoyan, Lattice methods for multiple integration: Theory, error analysis and examples, (1987), J. Numer. Anal., 24, 116-128.
- [19]. I.M. Sobol (1967), "Distribution of points in a cube and approximate evaluation of integrals". *Zh. Vych. Mat. Mat. Fiz.* **7**: 784–802 (in Russian); *U.S.S.R Comput. Maths. Math. Phys.* **7**: 86–112 (in English).
- [20]. Sobol, I. M. (1976) "Uniformly distributed sequences with an additional uniform property". *Zh. Vych. Mat. Mat. Fiz.* **16**: 1332–1337 (in Russian); *U.S.S.R. Comput. Maths. Math. Phys.* **16**: 236–242 (in English).
- [21]. I. Sobol', D. Asotsky, A. Kreinin, S. Kucherenko, "Construction and Comparison of High-Dimensional Sobol' Generators" , *Wilmott Journal. Nov*: 64–79, 2011.
- [22]. V. Todorov, I. Dimov, V. Dzurov, T. Stanchev, I. Tsvetkov, V. Dimitrov: A Numerical study on Hammersley sequence and Fibonacci based lattice rule for computation of multidimensional integrals, *Journal Scientific and Applied Research*, Vol. 12, 18-26, Konstantin Preslavsky Publishing House, ISSN 1314-6289, 2017.
- [23]. Y. Wang and F.J. Hickernell, An historical overview of lattice point sets, (2002).



## **APPLICATION OF AUTODESK SOFTWARE PRODUCT FOR TRAINING OF STUDENTS IN GENERAL ENGINEERING**

**Anton Antonov**

*KONSTANTIN PRESLAVSKY UNIVERSITY OF SHUMEN, FACULTY OF TECHNICAL  
SCIENCES, 115 UNIVERSITETSKA STR., 9712 SHUMEN, BULGARIA,  
E-mail: antonii\_a@abv.bg*

**ABSTRACT:** *One of the most complex and dynamic enterprise systems are logistics. The system designing requires many people, whereas specialized software products can be used to help design different elements and stages. Certain purpose of the work is to be presented software products Autodesk Factory Design Suite and their application in the education of the students in general engineering, which leads to break the traditional way of absorption the material. This cause lasting interest in science, which is a prerequisite for highly qualified personnel, competition in the labor market.*

**KEYWORDS:** *Autodesk Factory Design Suite, AutoCAD Mechanical, Autodesk Inventor, Learning students, Basic engineering*

### **1. Introduction**

One of the most complex and dynamic systems of an enterprise are logistics. They are composed of multiple elements with links between them as transport, warehouses for raw materials, manufacturing, warehouses and storage equipment for finished goods, shops and not least people.

System designing requires a lot of people, whereas specialized software products can be used to help design different elements and stages. One of the software that can be used to design systems like warehouse logistics, storage equipment, factory buildings and equipment, machinery and details is Autodesk Factory Design Suite.

Therefore the aim of the current work is to be presented the software products Autodesk Factory Design Suite and their application in the education of students in general engineering.

### **2. Exposition**

Autodesk Factory Design Suite is a package of many programs that are designed to create projects with maximum accuracy - from idea to implementation.

Autodesk Factory Design Suite has three versions: Standard, Premium and Ultimate. During the education, students use all three versions free.

During the education, students from Shumen University, Department "Logistics Engineering" use Autodesk Factory Design Suite Ultimate version 2017 and version 2018. The software package consists of AutoCAD Mechanical, AutoCAD Architecture, AutoCAD MEP, Autodesk Inventor Professional, Autodesk Navisworks Manage, Autodesk 3ds Max, Autodesk Vault, Autodesk Showcase, Autodesk Factory Design Suite Utilities, AutoCAD Raster Design and Autodesk ReC.

Stated software products can be used separately or in combination. They can create 2D and 3D digital models of the details and plans of warehouses, storage equipment, industrial plant and equipment in them. After creating the digital models with the software, they can perform simulations of different loads of detail, efficiency of warehouses and manufacturing plans. In engineering preparation of students, the informative approach is used. "Through this approach, learning of each object, process or phenomenon, students discover and analyze the characteristic information aspect, which is actually learning by analysis. This makes it possible to trace any integrity on the basis of the general to the specific, thus revealing information essence"[1].

In the teaching of students, who are specialized in class "Logistic Engineering" are often used "AutoCAD" and Autodesk Inventor in the specialties of "Simulation methods in designing logistic systems" and "Engineering graphics". Using AutoCAD Mechanical in the education of students is intended not only to produce 2D and 3D plans, but also in the process of training they learn to create design documentation to pick out ready plans, which have drawn details with real size which subsequently can be made (Figure 1).

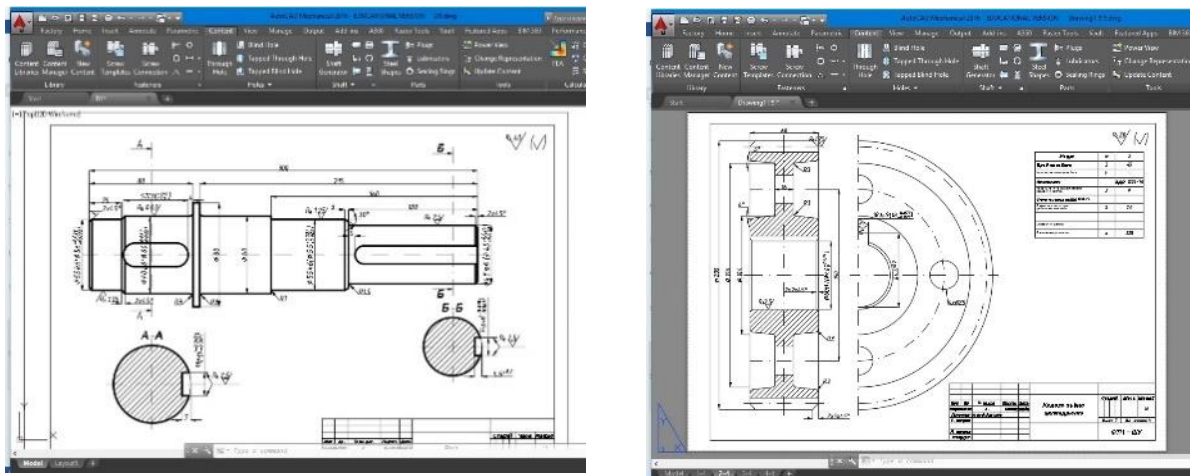
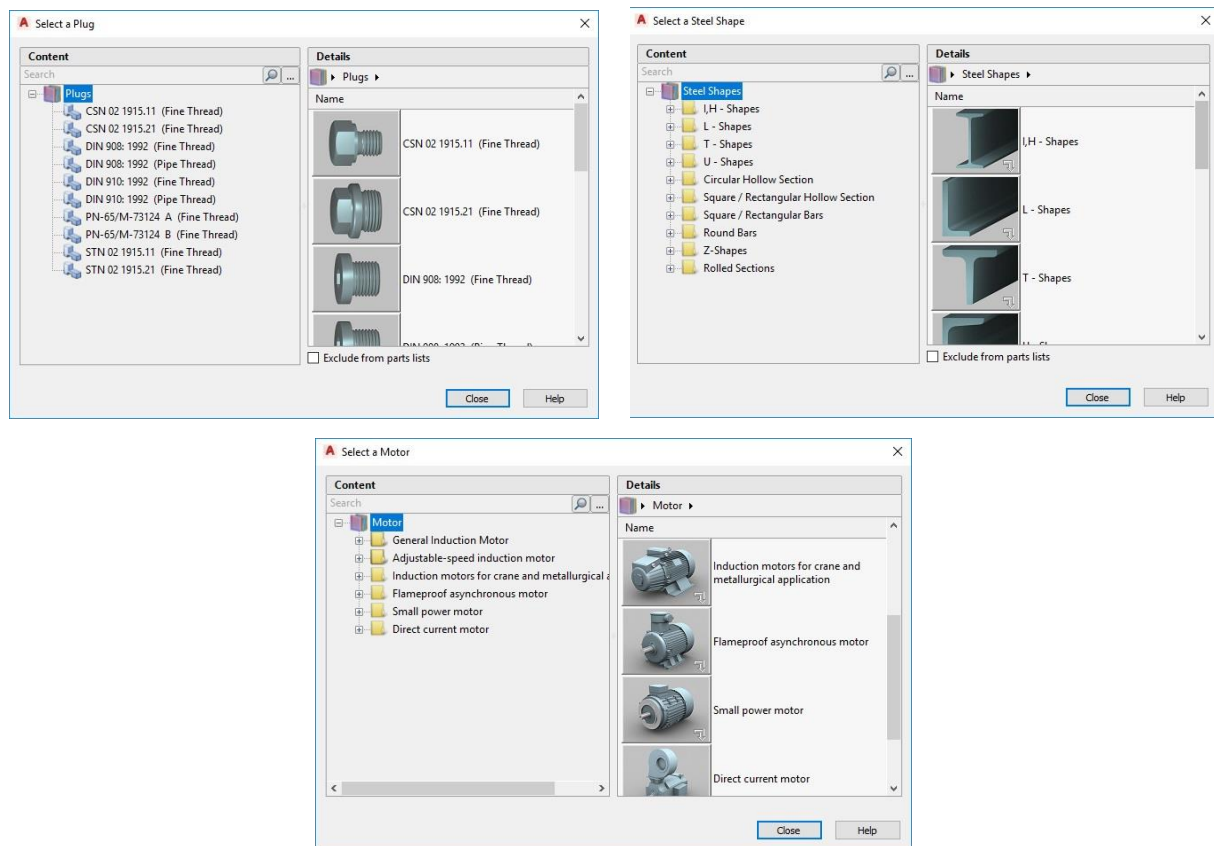


Fig. 1 Design Documents

AutoCAD Mechanical software is suitable for students with specialty “general engineering”, as it has built libraries with certified components to plot holes, carving joints, bearings, etc., Illustrated in Figure 2.



*Fig. 2. Libraries with standard components*

After completion of the course "Engineering Drawing" and acquaintance with AutoCAD Mechanical, students will be prepared to pick out and draw the design documentation, which will be of help for easy understanding of the material on subjects Mechanics, Machine Elements, Materials and others.

Another software product of the packet “Autodesk Factory Design Suite Ultimate”, which is used for educational purposes in teaching students, is Autodesk Inventor. It is taught the course "Simulation methods for designing logistics systems." It gives the students learn to design details, whole logistics systems and production facilities in 2D and 3D presented in the Figure 3[3, 8 ].

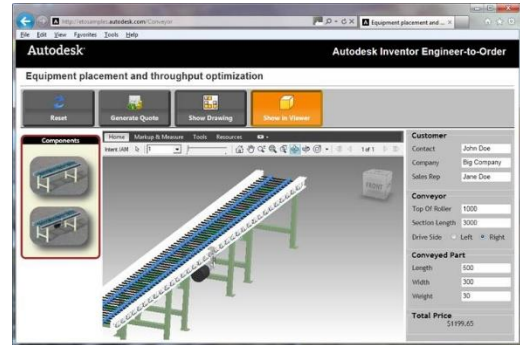
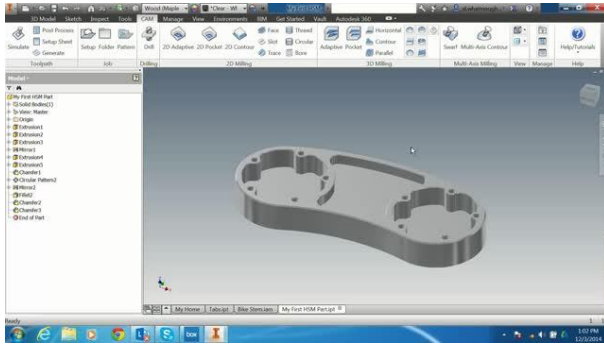


*Fig. 3. Design with Autodesk Inventor*

To help in the design of details and logistics systems come built into Autodesk Inventor libraries of standardized details, beams, tubes, ready units of conveyor belts, machines, manipulators, vehicles and more. Besides designing details, equipment, logistics systems and others with Autodesk Inventor can perform simulations and related resistance (strength loads) of parts, complete units and structures (Fig.4) [3, 9], which helps to reinforce the knowledge gained in other disciplines such as Mechanics, Machine Elements, Materials, etc. .

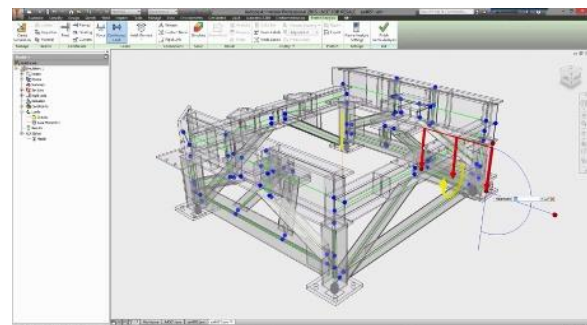
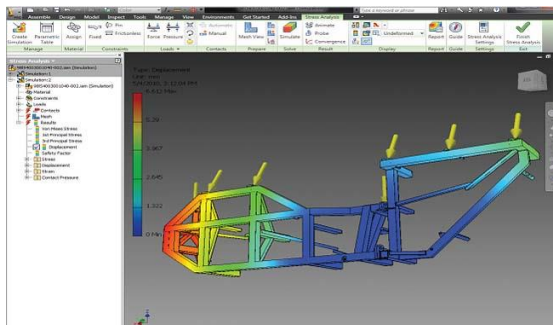


*fig. 4. Simulations of loads with Autodesk Inventor*

The teaching on "Simulation methods for designing logistics systems" except Autodesk Inventor considered and other programs included in the Factory Design Suite Ultimate -AutoCAD Architecture, AutoCAD MEP, Autodesk Inventor Professional, Autodesk Navisworks Manage, Autodesk 3ds Max, Autodesk Vault, Autodesk Showcase, Autodesk Factory Design Suite Utilities, AutoCAD Raster Design, Autodesk ReC.

With Reverse engineering Autodesk Inventor and other programs of Factory Design Suite, students acquire knowledge about design details, logistics and production systems. The knowledge will be helpful to the study of subjects "Courses of design" and "Engineering logistics systems"

### **3. Conclusion**

In conclusion it can be said that the application software of Autodesk Factory Design Suite in the training of students in general engineering breaks the traditional way of learning process. This cause lasting interest in science, leading to a highly qualified staff, competitors in the labor market.

### **References:**

- [1]. Dimitrova, N., Application of modern approaches for training of students. International Scientific Online Journal – ISSN 2367-5721 ISSUE 13, SEPTEMBER 2015 pp 18 – 21.
- [2]. G. Tonkov, Peykova M., On the advances of cad projecting in education. <http://www.mech-ing.com/journal/Archive/2010/1-2/>
- [3]. <http://www.autodesk.com/products>
- [4]. <http://help.autodesk.com/view/INVNTOR/2016/ENU/>
- [5]. <http://bmg.bg>
- [6]. <http://www.cadpoints.com/>
- [7]. <http://www.procad-bg.com/>
- [8]. <https://www.3dcadworld.com/autodesk-inventor-eto-gets-webified/>
- [9]. <http://old.digitaleng.news/de/fea-behind-the-scenes-of-machines/>



## DETERMINATION OF VISIBILITY BETWEEN CARD POINTS

**Sabin Ivanov**

*KONSTANTIN PRES LAVSKI UNIVERSITY OF SHUMEN, SHUMEN 9712, 115  
UNIVERSITETSKA STR.*

*E-mail: S.ivanov@shu.bg*

**ABSTRACT:** *The article discusses methods for determining visibility between two points of a topographic map. The different ways are depicted depending on what we have at our disposal.*

**KEYWORDS:** *visibility, altitude, exceedance, obstacle, sight beam*

Determining the visibility between two points can be done in several ways: comparing point heights by constructing a triangle, computing, and building a profile.

### 1. Determine visibility by comparing point heights.

- Explore the relief in the direction of the observed point and determine the unevenness that would interfere with visibility;
- Set the altitude of the starting point ( $H_{\text{start.}}$ ), the obstacle ( $H_{\text{obst.}}$ ) and the end point ( $H_{\text{end}}$ );
- Compare the determined altitudes Fig. 1 if:
  - $H_{\text{obst.}}$  is less than  $H_{\text{start.}}$  and  $H_{\text{end}}$ , then we have visibility;
  - $H_{\text{obst.}}$  is higher than  $H_{\text{start.}}$  and  $H_{\text{end}}$ , then we have no visibility;
  - $H_{\text{obst.}}$  is less than  $H_{\text{start.}}$  and higher than  $H_{\text{end}}$  or vice versa, the visibility is questionable. In this case, the distance between the obstacle and the end point affects visibility. As the obstacle is closer to the endpoint, the more it will interfere with the visibility, and vice versa, the longer the visibility is better.

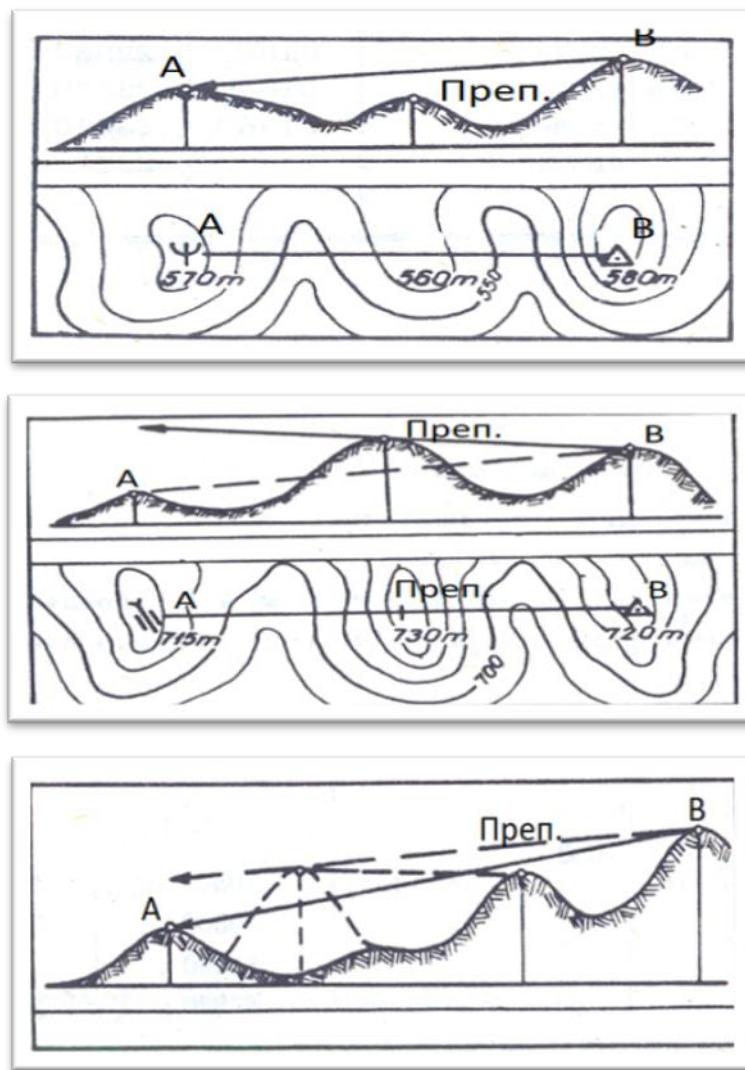


Fig.1. Altitude comparison

2. Identify visibility by building a triangle on the map.

- Joints with a straight line start and end point. On the same line, the obstacle point is noted, which will eventually hinder visibility;
- Determine the altitudes of the start, end and point of the obstacle ( $H_{start.}$ ,  $H_{end.}$  и  $H_{obst.}$ );
- The height of the lowest point is taken to zero and we calculate the excesses  $\pm\Delta h$  between it and the other two points. Excess is obtained as a difference in altitudes between two points;
- Calculated excesses on an appropriate scale are applied from the corresponding points perpendicular to the line connecting the starting point and the endpoints;
- The raised perpendiculars are connected with a straight line - a visual beam. If the beam passes over the point taken to zero, we have no visibility, and vice versa;

- To determine how many meters to climb for visibility, it is necessary to pass a second beam through the zero point and the perpendicular point raised from the obstacle point to cross the perpendicular to the rest of the point. On the perpendicular, the distance between the two beams is measured and the excess is determined.

Example: Determine the visibility between point A and point B by constructing a triangle on a topographic map on the scale M 1: 25000 fig.2.

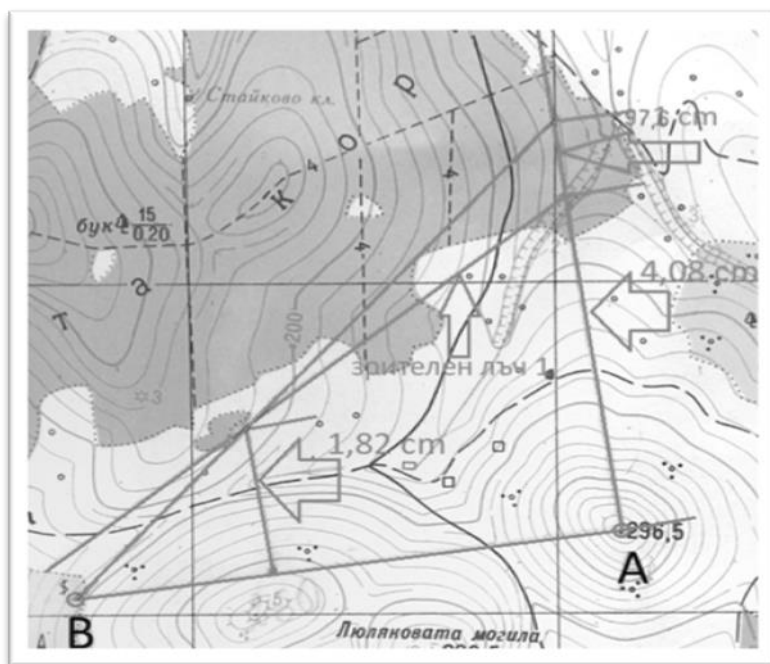


Fig.2. Determination of visibility by triangle

- We connect point A and point B. We apply the point of the obstacle;
- We set the altitudes:  $H_A(\text{startpoint}) = 296,5 \text{ m}$ ;  $H_B(\text{endpoint}) = 194,5 \text{ m}$ ;  $H_{\text{obst.}} = 260 \text{ m}$ ;
- We accept  $H_B = 0 \text{ m}$  (lowest point) and calculate:  $\Delta h_{BA} = 296,5 \text{ m} - 194,5 \text{ m} = 102 \text{ m}$ ;  $\Delta h_{B-\text{obst.}} = 260 \text{ m} - 194,5 \text{ m} = 45,5 \text{ m}$ .
- We divide the two excesses to 25 to get values that are convenient to map (if we divide by 100 or 50 we get very small numbers, so divide by 25):  $\Delta h_{BA} = 102 \text{ m} / 25 = 4,8 \text{ cm}$ ;  $\Delta h_{B-\text{obst.}} = 45,5 \text{ m} / 25 = 1,82 \text{ cm}$ ;
- Once we connect perpendiculars we see that we have no visibility (the sight beam passes over point B);
- After constructing the second beam and measuring the difference between it and the first (in this case 1 cm), we determine how much the height of the point A is to change in order to have visibility:  $\Delta h = 1 \text{ cm} * 25 = 25 \text{ m}$ .

### 3. Definition of visibility by calculation.

- Joints with a straight line start and end point. On the same line, the obstacle point is noted, which will eventually hinder visibility;
- Calculate the excess  $\Delta h$  between the start and the end point and  $\Delta h$  between the obstacle and the lower of the two (starting or ending);
- Measure the distance in cm between the starting point and the end point, and between the obstacle and the lower one (starting or ending);
- Two ratios are compiled - over-distances and distances;
  - exceedance -  $\Delta h$  between the start and end point to  $\Delta h$  between the obstacle and the lower of the two (starting or ending);
  - Distances - the distance in cm between the starting point and the end point to the distance between the obstacle and the lower one (starting or ending);
- Comparing both ratios. If the ratio of overshoots is greater than over-distances, we have visibility and vice versa.

Example: Determine the visibility between point A and point B by computing on a topographic map on scale M 1: 25000, fig.3.

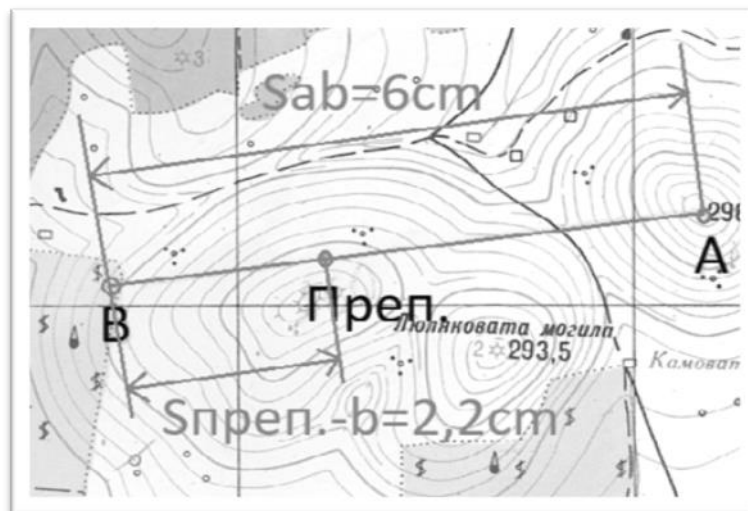


Fig.3. Definition of visibility by calculation

- We connect point A and point B. We apply the point of the obstacle;
- We calculate  $\Delta h_{BA} = H_A - H_B = 296,5 \text{ m} - 194,5 \text{ m} = 102 \text{ m}$ ;  
 $\Delta h_{B-\text{obst.}} = H_{\text{obst.}} - H_B = 260 \text{ m} - 194,5 \text{ m} = 45,5 \text{ m}$ ;
- We measure distances:  $S_{AB} = 6 \text{ cm}$ ;  $S_{\text{obst.}-B} = 2,2 \text{ cm}$ ;
- We draw up the ratios:
  - 1)  $102 \text{ m} / 45,5 \text{ m} = 2,24$ ;
  - 2)  $6 \text{ cm} / 2,2 \text{ cm} = 2,73$ ;
- It seems that the first attitude (the exceedance) is less than the second (distance), from which it follows that we have no visibility.

#### 4. Identify visibility by building an account.

Profile is called the vertical section of the area on the line between two points (profile line). Profiles are full and shortened.

- Full profile.

When building the full profile, all the heights on the profile line are used (basic, the additional, auxiliary horizons and altitude check markers).

The profile is built on a millimeter paper, and for a more accurate acquisition of the actual relief forms a suitable vertical scale is selected.

Order of operation, fig.4.

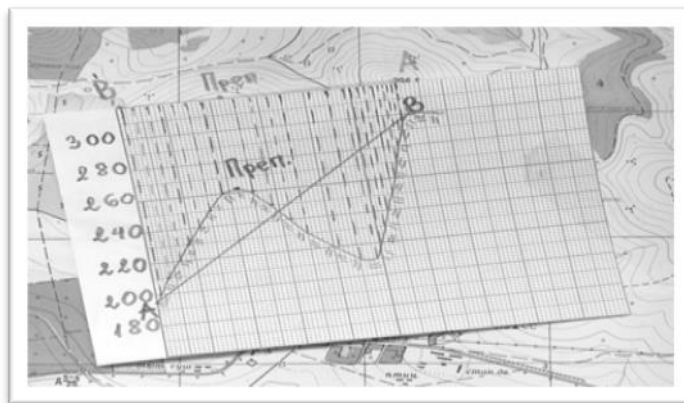


Fig.4. Build complete profile

- We connect with a straight line the start and the end point (profile line);
- In the left frame of the millimeter paper are inscribed (opposite the horizontal lines) the height of the horizons from the lowest to the highest height, along the line between the starting point and the end point (from bottom to top);
- Place the prepared millimeter paper on the line between the dots so that the top edge is on the line. From each intersection point of the line with the horizontal we drop perpendiculars to the corresponding inscribed horizontal lines of the millimeter paper;
- The points obtained are joined by hand with smooth lines.

- Short profile.

Building a shortened profile does not differ significantly from building a full profile. The difference is that the reduced profile on the millimeter paper transfers only the horizons expressing the ascent and descent boundaries, the sharp bends and the slopes, the horizons between them not being displayed.

### References

- [1]. Ivanov S. A guide for working with a topographic map, University Publishing Bishop Konstantin Preslavski, Shumen, 2018.
- [2]. Kastreva P., Geographic information systems and computer cartography, University Publishing Neofit Rilski, Blagoevgrad, 2011.



## **DETERMINING THE SCALE OF A TOPOGRAPHIC MAP**

**Sabin Ivanov**

*KONSTANTIN PRES LAVSKI UNIVERSITY OF SHUMEN, SHUMEN 9712, 115  
UNIVERSITETSKA STR.*

*E-mail: S.ivanov@shu.bg*

**ABSTRACT:** *The article shows all methods for determining the scale of a topographic map. the methods shown can be used when the scale is not displayed on the map.*

**KEYWORDS:** *scale, map, numerical scale, graphical expression.*

### 1. General considerations.

To be able to measure distances from the map and solve a number of practical tasks, we need to know its scale.

Scale of the map is called the ratio of the lengths of the lines of the map to the horizontal lengths of the same lines from the area:

$$(1) \quad \frac{a}{A} = \frac{1}{M}$$

where:  $a$  - the measured distance from the map (recorded in meters),  $A$  - the same distance of the area;  $M$  - Scale.

On each map the scale is written under the southern frame in the middle of the card sheet and is expressed numerically and graphically (linear) Fig.1.



Fig.1. Numerical, graphical scale and scale number

Numerical scale is called the scale expressed by the relation between the number 1 and the number, which shows how many times the lengths of the lines of the locality have been reduced when displayed on the map. Example: 1: 10000; 1: 50000; 1: 1000000.

When using the numeric scale, when we measure a distance from the map, the centimeters and millimeters we read are multiplied by the scale corresponding to 1 cm in the scale of the map. On most maps, this value is labeled below the numerical scale. If there is no inscription, the easiest way is the so-called "rule of the two zeros" fig.2. Example: if the scale is 1: 25000, hiding the last two zeros with the finger, we get that 1 cm of the map corresponds to 250 m from the area.



Fig.2. "Rule of Two Zeros"

Linear scale is called the graphical expression of numerical scale. It is a straight line, divided into equal divisions, which correspond to a certain circular number of meters from the area for the given scale fig.3.

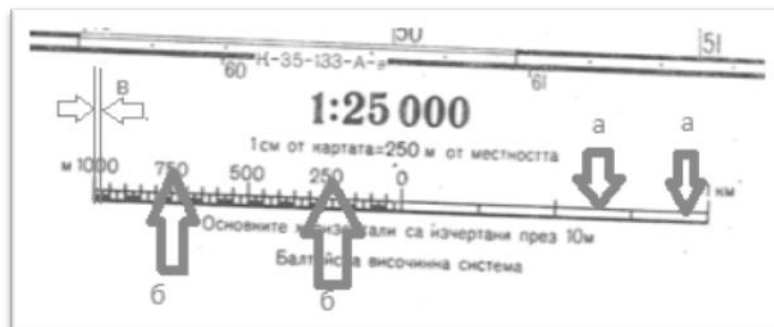


Fig.3. Linear scale

- a - basis of the linear scale - the largest division, expressed in centimeters;
- b - magnitude of the linear scale - the number of meters from the area corresponding to the base;
- in - linearity accuracy - the number of meters from the site corresponding to the smallest scale scale to the left of zero.

## 2. Determining the scale of the map.

If the scale of the card is missing or not specified, then it can be determined in one of the following ways:

- On the map nomenclature - Each scale has its strictly defined nomenclature - Table 1.

Table 1

Мащаб	Означение
1 : 1 000 000	К-34
1 : 500 000	К-34- А, Б, В, Г
1 : 200 000	К-34- I, II, ..., XXXVI
1 : 100 000	К-34- 1, 2, 3, ..., 144
1 : 50 000	К-34-45- А, Б, В, Г
1 : 25 000	К-34-45-Б- а, б, в, г
1 : 10 000	К-34-45-Б-б 1, 2, 3, 4
1 : 5 000	К-34-45 (1, 2, 3, ..., 256)
1 : 2 000	К-34-45 (235-а, б, в, ..., и)

- The kilometer (coordinate) network.

Example: The square of the grid is 4 cm and the gauge is passed through 2 mm. The scale is defined as follows:

4 cm of the map corresponds to 2000 meters from the area.

1m of the map corresponds to Xm from the area.

$$(2) \quad X = \frac{2000 \cdot 1}{4} = 500m$$

$$M = 1:50000$$

- The milestones along the roads.

Example: The distance between two neighboring milestones on the map is 2 cm (Fig.4). What is the scale of the map?

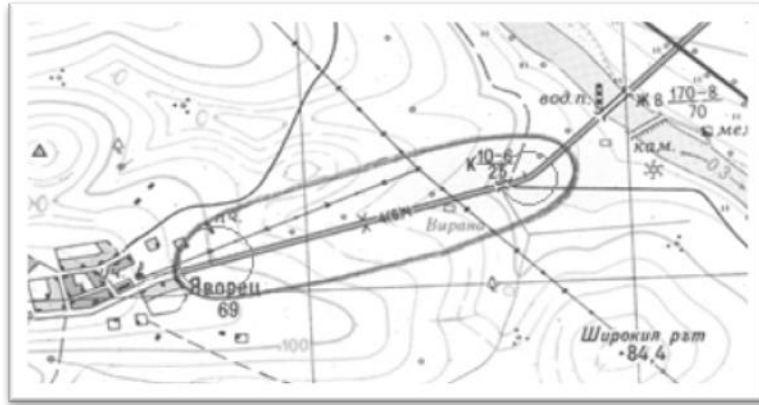


Fig.4. Kilometric stones

Two centimeters of the map correspond to 1000 m of the area.  
 1m of the map corresponds to X m from the area.

$$(3) \quad X = \frac{1000 \cdot 1}{2} = 500m$$

$$M = 1:50000$$

- Measured distance of the area.

We measure the distance between two typical local objects in meters that are mapped to the map. From the map we measure the same distance in centimeters.

Example: The distance between road bridge and roadside fountain is 850 m, and the same distance on the map is 3.4 cm.

3.4 cm of the map corresponds to 850 meters from the area.  
 1m of the map corresponds to X m from the area.

$$(4) \quad X = \frac{850 \cdot 1}{3,4} = 250m$$

$$M = 1:25000$$

- By comparing the same distance on another map of a certain scale.

Example: On a map in M 1: 50000 the distance between a transformer and a road junction is 8.6 cm. The same distance between the two objects on another map of unknown scale is measured 4.3 cm.

$$8,6 \text{ cm} \times 500 = 4300 \text{ m}$$

На 4,3 см от картата отговарят 4300 м от местността.

На 1 см от картата отговарят X м от местността.

$$(5) \quad X = \frac{4300 \cdot 1}{4,3} = 1000m$$

$$M = 1:100000$$

- On the length of the arc for one minute on the meridian.

The length of one minute on the meridian is about 1852.2 m and is equal to one nautical mile. On the eastern and western frames of each topographic map, the meridian minutes are mapped on a large scale (Fig.5). The scale of the map is obtained by dividing the length of the corresponding distance from the area corresponding to the minutes in centimeters of the map.

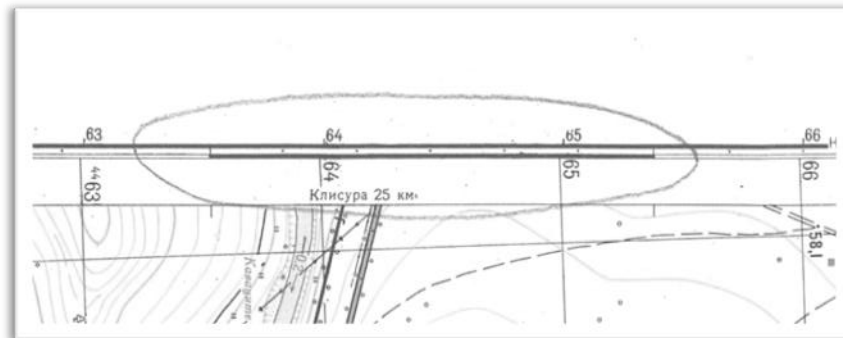


Fig.5. Minute on the meridian

Example: The length of one division is 5 minutes along the meridian of the map and is equal to 4.63 cm. The same distance from the site will be:  $5 \times 1852,2 = 9261$  m.

At 4.63 cm of the map correspond to 9261 meters of the area.

1 cm of the map corresponds to X m from the area.

$$(6) \quad X = \frac{9261.1}{4,63} = 2000m$$

$$M = 1:200000$$

## References

- [1]. Ivanov S. A guide for working with a topographic map, University Publishing Bishop Konstantin Preslavski, Shumen, 2018.
- [2]. Kastreva P., Geographic information systems and computer cartography, University Publishing Neofit Rilski, Blagoevgrad, 2011.



## ESOPHAGEAL CARCINOMA AND BLOOD GROUP AFFILIATION

**Velislav Todorov, Maria Boycheva\*\*, Volodia Georgiev\*, Cvetan Minkov,  
Milen Boichev\*\*, Rada Georgieva**

*SOFIA UNIVERSITY, FACULTY OF BIOLOGY, DEPARTMENT OF ZOOLOGY AND ANTHROPOLOGY, \*DEPARTMENT OF GENETICS, 8 DRAGAN TZANKOV STR., SOFIA, BULGARIA*

*\*\*KONSTANTIN PRES LAVSKY UNIVERSITY OF SHUMEN, FACULTY OF NATURAL SCIENCE, DEPARTMENT OF BIOLOGY, 115 UNIVERSITETSKA STR, SHUMEN, BULGARIA*

**ABSTRACT:** *The article describes a study of 92 patients (79 male and 13 female) with esophageal carcinoma - Ca oesophagii. The patients' blood type affiliation to ABO and Rhesus factor systems was established. In comparison with the control group, consisting of healthy representatives of modern Bulgarian population, there was a statistically significant increase of disease incidence in patients with blood type A (by 22,60% to 66,30%) -  $P < 0.05$ . In patients with other blood types there was a varying decrease of incidence (more pronounced in groups O and B). Significant sex-based dimorphism was observed in the distribution of the disease in the studied sample (predominantly male patients). We assume that blood type A affiliation is one of the risk factors for the development of this disease. In the Rhesus Factor system there were no differences between the studied sample and the control group.*

**KEY WORDS:** *blood groups ABO and Rhesus factor, Ca oesophagii*

**Introduction:** A great deal of our previous research has been concerned with the possible correlation between blood group affiliation and human diseases. We have studied both benign and malignant diseases, while focusing in particular on carcinomas. We believe there may be a link between the onset and progression of diseases and certain biological factors, namely the blood group affiliation of the patients. So far, we have tracked and demonstrated some interrelations between blood type and carcinoma of the female reproductive system, such as (Ca ovarii, Ca uteri, Ca glandulae mammae) [1], (Ca vulvae) [2], the male reproductive system (Ca glandulae prostatae) [1], (Ca penis, Ca testis) [3], the urinary tract (Ca renis) [4], (Ca vesicae urinariae) [5], the respiratory system (Ca pulmonis) [6], and the skin (Melanoma maligna) [7].

**Aim of the study:** To establish whether there is a link between the blood type affiliation of patients to the AB0 and Rhesus factor systems and the appearance and development of Ca oesophagii.

**Material and methods:** 92 patients (79 men and 13 women) with esophageal carcinoma (Ca oesophagii) were studied. The patients were diagnosed and treated in the Oncology Ward of the Fifth Hospital in Sofia. Their blood group affiliation to the AB0 and Rhesus factor systems was compared with the control group of healthy persons of Bulgarian population [8] using the  $\chi^2$  criterion.

**Results and discussion:**

The data of the study are presented in table 1 and figure 1 and 2.

Table 1. Frequency of the blood types from systems AB0 and Rhesus factor in patients with Ca oesophagii and the control group (%).

Blood types		O	A	B	AB	Rh+	Rh-
Patients with Ca oesophagii n 94	n	19	61	6	6	79	13
	%	20,66	66,30	6,52	6,52	85,87	14,13
Control group n 1080	n	342	472	184	82	916	164
	%	31,67	43,70	17,04	7,59	84,81	15,19

AB0 system

In the studied patients with Ca oesophagii the following distribution of the frequencies of the individual blood types was established: type O - 20,66%, type A - 66,30%, type B - 6,52%, and type AB - 6,52%. In the control group the values were: type O - 31,67%, type A - 43,70%, type B - 17,04%, and type AB - 7,59%, respectively. The comparison between groups showed a significant increase in the incidence in patients with type A (by 22,60% to 66,30%) -  $p < 0.05$ , and a varying decrease of the values in the other blood types (in type B - by 11,54%, in type O - by 11,01%, and in type AB - by 1,07%). The observed differences are not significant -  $p > 0,1$  (table 1 and figure 1).

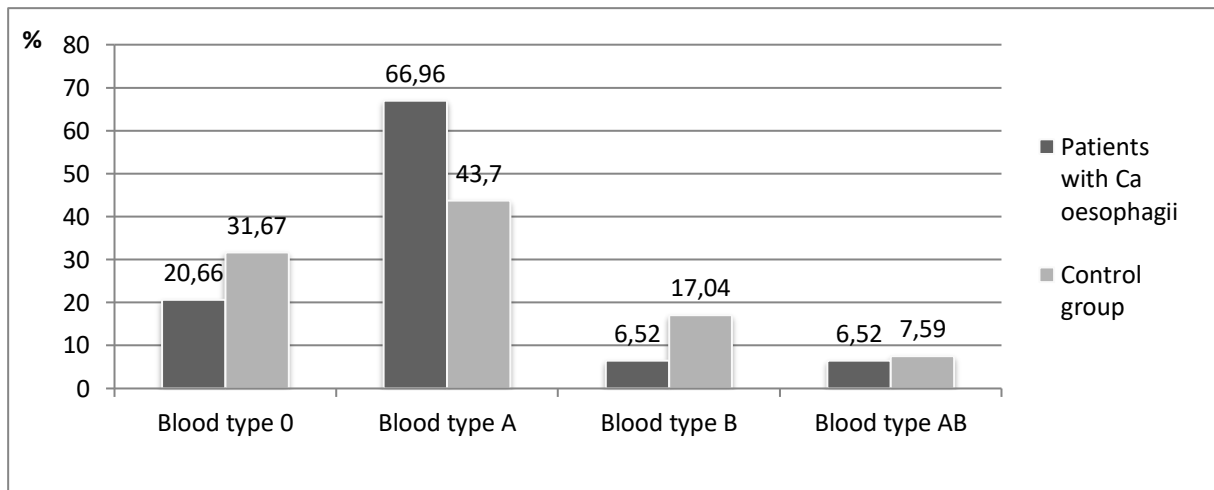


Figure 1. Frequency of the blood types from system ABO in patients with Ca oesophagii and the control group (%)

### Rhesus factor system

The frequencies of the two types of this system in patients with Ca oesophagii were 85,87% Rh+ and 14,13% Rh- , respectively. In the control group, the values were 84,81% and 15,19%, respectively. There were no differences in the values between the studied patients and the control group of healthy persons of Bulgarian population (Table 1 and Figure 2).

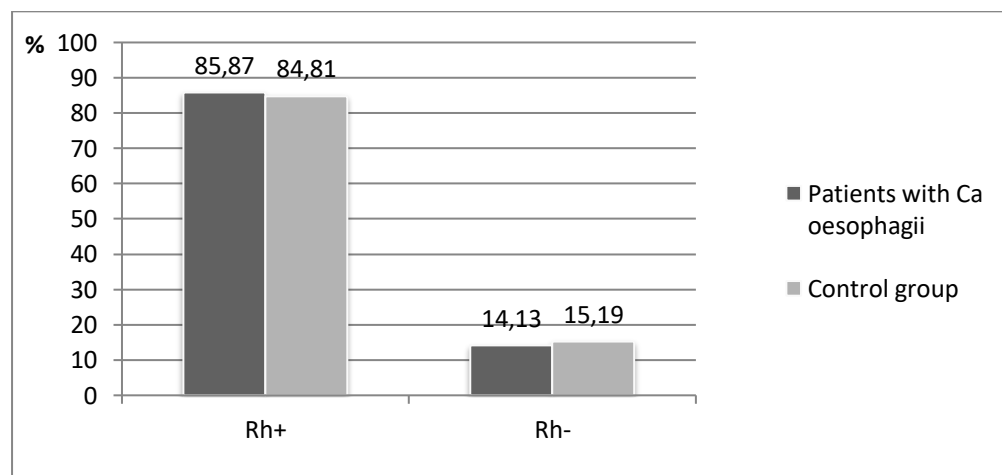


Figure 2. Frequency of the blood types from system Rhesus factor in patients with Ca oesophagii and the control group (%)

Oesophageal carcinoma is the eighth most frequent carcinoma worldwide with a late clinical manifestation, relatively ineffective therapy, poor prognosis, and high mortality [9, 10].

There are two main forms of this carcinoma - squamous cell carcinoma and adenocarcinoma [10]. The first form occurs more often in less developed countries, while the second is more frequent in developed countries [9]. The risk factors for the development of squamous cell carcinoma are smoking and alcohol [9]. Smoking accounts for 50% of cases, and alcohol for about 33%, while the combination of the two - for 75% of cases [11, 12]. Adenocarcinoma risk factor is the prolonged acid reflux [13]. Smoking can also trigger its appearance [11]. It may also be due to other risk factors such as obesity [14]. Erosion processes due to acid reflux occur 20 years later in women than in men, probably due to hormonal factors. The impact of obesity is well manifested (20-30% of patients), but it is not quite clear how it affects the disease [13, 12]. Adenocarcinoma tends to increase in the western world, whereas the squamous cell carcinoma does not show a change in frequency [15].

The highest incidence of adenocarcinoma is observed in Northern and Western Europe (Great Britain, the Netherlands, Ireland and Spain), and New Zealand [16]. For example, in the United Kingdom, the incidence is 18/100000 in the male population and 8.5 / 100000 in female. In this country, 83% of the patients are over 60 years old, and 42% are over 75 years old [10, 14].

Worldwide, the incidence of this disease is 5.2/ 100,000, with pronounced gender differentiation - 7.7 / 100,000 in males and 2.8 / 100,000 in females [16].

The incidence of Ca oesophagii in our country is 2.6/100,000, representing 0,5% of all oncological diseases. There is a marked gender difference in the prevalence of the disease. For the males the values are 4.3/ 100000 – 0,9%, and for the females they are 1.0/ 100000, which is 0,3% [17]. The ratio between the two sexes corresponds to this distribution (85,39% for men and 14,61% for women).

In most of the malignancies covered by us, a significantly higher incidence of blood type A patients compared to the control group [8] has been reported so far. These involve the carcinomas Ca uteri -  $p < 0.01$ , Ca ovarii -  $p < 0.01$ , Ca glandulae mammae -  $p < 0.01$ , Ca glandulae prostatae -  $p < 0.01$  [1], Ca pancreatis  $p < [18]$ , Ca penis -  $p < 0.001$ , Ca testis -  $p < 0.001$  [3]. In Ca ventriculi and Ca coloni, there was a certain increase in group A, but without significant differences [1]. Some carcinomas - Ca vulvae -  $p < 0.05$  [2] and Ca renis -  $p < 0.001$  showed a significant increase in blood type 0 [4].

Some authors believe that there might be genetic factors which trigger the onset and development of the disease [10].

There are three main stages in the development of the esophageal tumor [10] - T, N, M:

T - primary tumor with seven sub-stages;

N - Metastasis in the lymph nodes with three sub-stages;

M - distant metastases with three sub-stages.

The treatment of this disease involves radiotherapy, combined radiotherapy and chemotherapy, laser therapy, endoscopic prosthesis, and rarely - surgical intervention. Different types of procedures are performed depending on the type and stage of the disease [10].

Our study of the blood type of the patients and the significant increase of disease in patients of type A gives us reason to assume that this blood type is one of the genetic risk factors for the development of the disease.

### **Conclusions:**

1. In the ABO blood type system of the studied patients there was a significant increase in blood type A ( $p < 0.05$ ) patients, compared to the control group.

2. We assume that blood type A is one of the genetic factors for the appearance and development of esophageal carcinoma.

### **References:**

- [1]. Maksimova, S., V. Todorov, A. Timceva. Sistema krvnih grupa ABO i Resus factor kod nekih oboljenja od socijalnog znacaja, Glasnik antropoloskog drustva Jugoslavije, 1997, 33, 119-124.
- [2]. Todorov, V., S. Maksimova. Krvnogrupni sistemi ABO I Rh factor kod pacijenkinja sa karcinomom vulvae, Glasnik antropoloskog drustva Srbije, 2011, 46, 179-181.
- [3]. Maksimova, S., V. Todorov, K. Yanev, P. Panchev. Novoobrazuvaniya i krvnogrupova prinadlezhnost kam sistemite ABO i Resus faktor. Andrologia, 2009, 4, 9-11.
- [4]. Todorov, V., S. Maksimova, V. Hristova. Kartsinom na babreka i krvnogrupova prinadlezhnost, Andrologia, 2008, 2, 12-13.
- [5]. Todorov, V., S. Maksimova, V. Hristova. Karcinom mokracne besike i krvne grupe, Glasnik antropoloskog drustva Srbije, 2008, 43, 72-74.
- [6]. Todorov, V., M. Boychev, V. Georgiev, Tz. Minkov, N. Paraskova. ABO and Rh factor blood group frequencies in patients with lung cancer, Journal education innovation, 2015, 4, 74-77.
- [7]. Todorov, V., M. Boychev, Tz. Minkov, V. Georgiev, N. Paraskova, M. Boycheva. Blood group affiliation in melanoma maligna patients, Journal scientific and applied research, 2015, 8, 41-46.
- [8]. Todorov, V. Promene antropoloskih karakteristika u toku starenja, Disertacija doktora nauka, Beograd, 1998-1999, 72-77.
- [9]. Montgomery, E. Esophageal cancer in Stewart, BW, Wild, CP., World Cancer Report 2014, World Health Organization, 528-543.

- [10]. Vladimirov, B. Rak na hranoprovoda, gastroezofagialnata vruzka i stomaha. *Bulgarska gastroenterologia*, 2006, 14-26.
- [11]. Rutergard, M., P. Lagergre, N. Nordenstend, I. Lagergren. Oesophagial adenocarcinoma: the new epidemic in men? *Maturitas* 69(3):244-8. doi:10.1016/j.naturitas.2011.04.003, PMID 21602001.
- [12]. Cantelucia, V., D. Sanaonno, G. Ingravallo, S. Marangi, S. Russi, G. Lauletta, F. Dammacco. Barrett's oesophageal cancer: An overview. *International Journal of Oncology* 41(2),414-424. doi: 10.3892/ijo.2012.1481, PMID 2261501.
- [13]. Lagergren, I. Influence of obesity on the risk of oesophageal disorders. *Nature Reviews. Gastroenterology&Hepatology* 8(6):340-7. doi:10.1038/nrgastro.2011.73.
- [14]. Calle, E. E., C. Rodrigues, K. Walker-Thurmond, M. J. Thun. Overweight, Obesity, and Mortality from Cancer in a Prospectively Studied Cohort of U.S. Adults, *N Engl J Med*, 2003, 348:1625-1638.
- [15]. Tobias, J. S., D. Hochhauser. *Cancer and menadement* (6<sup>th</sup> Ed), Wiley-Blackwell, 254.
- [16]. Arnold, M., I. Soerjomataram, I. Ferlay, D. Forman. Global incidence of oesophageal cancer by histological subtype in 2012. *Gut*.2015Mar; 64(3):381-7. doi: 10.1136/gutjnl-2014-308124, PMID 24320104.
- [17]. Dimitrova, N., M. Vukov, M. Valerieva. *zabolevaemost ot rak v Bulgaria*. *Natsionalna bolnitsa po onkologia*, 2013, 22, 60.
- [18]. Todorov, V., S. Maksimova. Povezanost izmedu krvnih grupa AB0 I Rh sistema i pojave carcinoma pancreasa, *Glasnik antropoloskog drustva Srbije*, 2010, 45, 187-190.

*The present study is conducted with the financial help of Project № ПД-08-167/09.02.2018, fund "Scientific studies" of Konstantin Preslavsky University of Shumen.*



## **HEAT – MECHANICALLY INDUCED STRUCTURE DEVELOPMENT IN PARTIALLY CRYSTALLINE POLYESTER FIBERS. INFLUENCE OF THE MECHANICAL STRESS**

**Valentin Velev<sup>1</sup>, Nina Arhangelova<sup>1</sup>, Daniela Nedeva<sup>2</sup>, Zhenya Stoyanova<sup>1</sup>,  
Anton Popov<sup>3</sup>**

<sup>1</sup>*KONSTANTIN PRES LAVSKY UNIVERSITY, 115 UNIVERSITETSKA STR.,  
9700 SHUMEN, BULGARIA  
E-mail: v.velev53@gmail.com; n.arhangelova@shu.bg*

<sup>2</sup>*TECHNICAL UNIVERSITY OF GABROVO, 4 HADJI DIMITAR STR.,  
5300 GABROVO, BULGARIA  
E-mail: nedeva.d@abv.bg*

<sup>3</sup>*UNIVERSITY "PROF. DR. ASSEN ZLATAROV",  
8000, BURGAS, BULGARIA  
E-mail: apopov1948@abv.bg*

**ABSTRACT:** *There are present results from high temperature uniaxial extension of partially crystalline poly (ethylene terephthalate) (PET) yarns. Effect of the applied to the samples tensile stress at isothermal conditions on the structural changes in the studied objects have been investigated. The structural analyses of the processed fibers were realized using differential scanning calorimetry (DSC).*

**KEYWORDS:** *polyester fibers, orientation extension, isothermal conditions, tensile stress, differential scanning calorimetry.*

### **1. Introduction**

As it is known the mechanical properties of the non-isotropic polymer systems strongly depend on their super molecular structure. Flexible chain polymer products are typically used in one- and two-axis oriented states in which they acquire improved deformation-strength performance. The wide application and consequently higher production of fiber forming polymers, in particular poly (ethylene terephthalate) (PET), is due to the possibility for additional treatments with purpose to obtain highly modular and high strength materials from them.

One of the main methods for improving of the mechanical properties of the oriented polymer materials is the heat-mechanical modification (HMM) in its various varieties [1-5]. A frequently used variant of HMM is the orientational high-temperature extension, which results in repackaging and in mutual parallel alignment of the macromolecular chain segments and improvement of the deformation-strength characteristics of the polymer system. The effectiveness of such a structural reorganization depends mainly on the properties of the primary polymer structure, and of the conditions of the non-destructive orienting download.

Therefore the necessary and sufficient condition for optimizing of the orienting extension is to find a science-based options to improve the mechanical properties on the flexible chain polymers in oriented state is the finding of a mutually suitable structures and conditions for their orientation downloading. On one side, finding of suitable of appropriate starting structure with a good deformability to achieve of maximum possible for a given polymer, non-destructive levels of orientational extension. On the other hand, finding of suitable conditions for achievement of maximum possible non-destructive levels of orientation download. Each structure requires the appropriate conditions for optimal downloading and specified downloading conditions are optimally suitable only for a single corresponding structure.

All of the above noted is particularly important for polyethylene terephthalate because of its great industrial production and wide application, mainly in oriented state. The crystallising PET is a model fiber forming complex two-phase (from a strictly physical point of view - multiphase) amorphous-partially crystalline system. The PET properties are strongly dependent on its degree of crystallinity as well as on the crystalline phase perfection. Therefore the studying actuality of the possibility for optimizing of its orientation download is indisputable.

## **2. Experimental**

### **2.1. Materials and Methods**

Partially crystalline PET as-spun multifilament yarn named S<sub>2</sub>, have been selected as a precursor sample.

The initial characteristics of the studied PET fibers were as follows:

- ✓ speed of fibrillate 2805 *m/min*;
- ✓ number of single filaments in the complex thread 32;
- ✓ diameter of a single fibre 13,0  $\mu\text{m}$ ;
- ✓ degree of crystallinity  $\alpha = 28,8 \%$ ;
- ✓ birefringence  $\Delta n \cdot 10^3 = 5,35$ .

Heat-mechanical treatment of the samples was carried out using a device for thermo-mechanical modification of orientated polymer materials, designed

and made in the author's laboratory. The studied PET yarns were performed under isothermal conditions at temperatures of 80°C and 85°C, in a narrow temperature range closely above their glass transition temperature [6].

The sample HMM includes annealing of PET fibers for ten minutes at the appropriate temperature, after that they are subjected for 120 seconds at the same temperature, to a well-defined tensile stress with values 40 MPa, 80 MPa and 120 MPa. The effects of some basic parameters of the HMM such as strain force, extension rate and temperature on the structure development of PET have been studied using different methods but most often differential scanning calorimetry (DSC).

Structural changes in the treated samples were examined using a differential scanning calorimeter DSC "Mettler Toledo" – 820. In accordance with the requirements of the DSC analyzes [7], the studied fibers were cut into parts less than one millimeter in length.

## 2.2. Results and discussion

The obtained DSC thermograms of the untreated sample S<sub>2</sub> as well as of the high temperature modified at a temperature of 80°C and under applied strain stress of 40 MPa, 80 MPa and 120 MPa are shown in Fig. 1.

As can be seen from Fig. 1, the effect of the tensile stress of 40 MPa is expressed in the narrowing of the multiple melting peak and the disappearance of the low temperature asymmetry in the melting peak of the untreated sample.

The most likely causes of the observed effect are as follows:

- ✓ homogenization of the fiber structure as a degree of orientation;
- ✓ unification of the packing density of the macromolecular chain segments.

As proof of this is the appearance of low-temperature melting phase, instead of the wide spectrum of fractions, that are responsible for the observed left asymmetry in the melting peak.

In combination with the observed fraction which melts at medium temperatures (Fig. 1), and with which overlaps strongly, the low temperature melting phases include within themselves the major amount of the polymeric material. Together with the fraction that melts at medium temperatures (Fig. 1), the phases that melt at lower temperatures include themselves the major amount of the polymeric material. At the same time, the quantitative reduction of the highest temperature-melting phase, indicates that the modification of the fiber under these conditions somewhat defects the polymer. Perhaps partial destructive processes affect this most ordered and pre-stressed structural part of the material.

At a strain stress of 80 MPa (Fig. 1) the high temperature melting phase recovers and even significantly exceeds quantitatively the high temperature melting phases of the untreated and less-oriented samples.

DSK curve obtained under strain stress of 120 MPa (Fig. 1) shows that the melting peak visible almost lost its multiple character. This may be a result of maximum compaction of the substance or overlapping of the phases and their reorganization in a single phase.

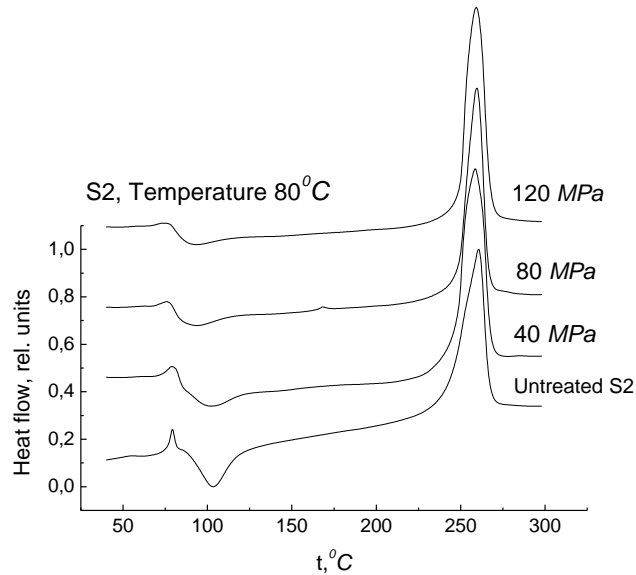


Fig. 1. DSC curves of PET fibers, heat mechanically modified at 80°C and values of the applied tensile stress of 40 MPa, 80 MPa and 120 MPa.

Probably, this phase is characterized by a close enough distribution between the molecular contacts of interaction energy, which is related to a narrow distribution of the macromolecular segments in the amorphous regions by degree of tautness.

The results of the DSC analyzes of sample S<sub>2</sub> subjected to HMM under conditions described above and temperature 85°C are shown in Fig. 2. As it can be seen from Fig. 2, with the increasing of HMM temperature up to 85°C, immediately at a tensile stress of 40 MPa there is observed a marked reduction in the width and asymmetry of the multiple melting peak.

Typical here is that even at this first, lowest strain load at HMM, the multipurpose structure of the composite peak almost disappears. This shows a strong compaction and alignment of the packaging of the macromolecular chain segments with low presence of left asymmetry and the existence of a low temperature-melting fraction.

With increasing of the orientation strain stress up to 80 MPa, at the same temperature of the object elongation (Fig. 2), the observed trend of stacking, respectively sealing of the packaging segment is preserved. It is observed a further reduction of the half-width of the composite melting peak which looks

almost symmetrical. Low temperature asymmetry has disappeared, and peak narrowing corresponds with its little deviation to the higher temperatures to the right on the temperature scale.

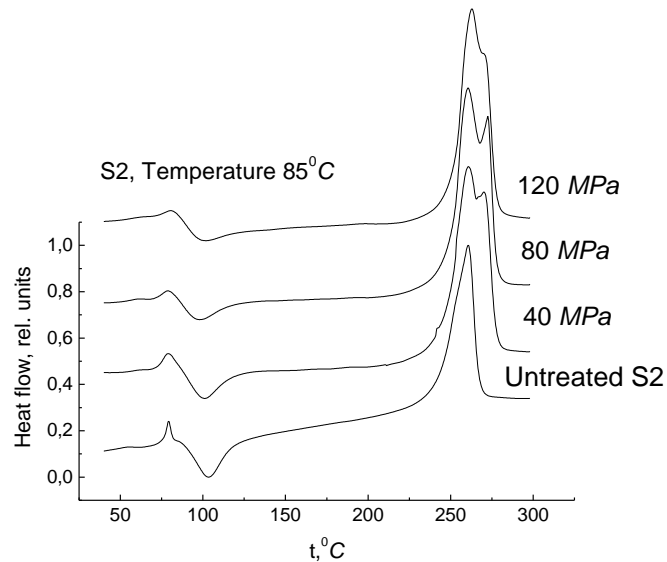


Fig. 2. DSC curves of PET fibers, heat mechanically modified at 85°C and values of the applied tensile stress of 40 MPa, 80 MPa and 120 MPa.

It can easily be assumed that the packing of the macromolecular chain segments of PET into the amorphous areas requires more heat energy, at a higher temperature to break intermolecular contacts and melt the material.

Increasing of the load to the maximum experimental of 120 MPa orientation tensile stress (Fig. 2) confirms the same, but less noticeable trend. In addition, there is observed a very low reverse position deviation of the melting peak on the temperature scale. Probably also in this case the highest mechanical load values, along with the high temperature of the modification, cause destructions that breaks the packaging of the macromolecular chain segments.

In conclusion, it is possible to note the deterministic influence of the orientation mechanical stress on the structural reconstruction of PET fibers in the isothermal modification mode.

On the other hand makes an impression the ambiguous role of its growth on the order increasing, homogeneity and consolidation of the structural organization of the objects. The above is based on the observed change in the quantitation ratio between the phases with different melting temperatures in the multiple melting peaks.

The observed effects are a logical consequence of the complex superposition of the alternative and mutually dependent competitive processes

of orientation and destruction, defining the mechanism of the high temperature orientation extension.

**Acknowledgment.** Part of the present work has been supported by Grants № ПД-08-142/08.02.2018 from Konstantin Preslavsky University, Shumen.

### **Conclusion**

Partially crystalline polyethylene terephthalate fibers were subjected to a high temperature orientation elongation. Samples were subjected to strain stresses of 40 MPa, 80 MPa and 120 MPa at temperatures of 80°C and 85°C.

Structural changes in the treated objects were studied using differential scanning calorimetry.

It was found that the orientation mechanical stress has a decisive influence on the structural changes of PET fibers in the isothermal mode of modification.

A satisfactory explanation of the obtained results needs of additional investigations and they are coming.

The planned next step of the studies, concerning the structural changes in PET filaments caused by heat-mechanical modification, includes fibers treatment at elevated temperatures of 90°C and 95 °C.

### **References**

- [1]. Anita Quye, Factors influencing the stability of man-made fibers: A retrospective view for historical textiles, *Polymer Degradation and Stability*, 2014, 107, 210 – 218.
- [2]. Ciardelli F., Ruggeri G., Pucci A., Dye-containing polymers: methods for preparation of mechanochromic materials, *Chemical Society Reviews*, 2013, 42, 857-870.
- [3]. Mercier J. P., Zambelli G., Kurz W., Introduction to Materials Science, *Elsevier*, 2012, p. 460.
- [4]. Karl F. J., High Performance Polymers, *William Andrew*, 2014, p. 440.
- [5]. Ayman A. Aly, Heat Treatment of Polymers: A Review, *International Journal of Materials Chemistry and Physics*, Vol. 1, No. 2, 2015, pp. 132-140.
- [6]. Velev V., Dimov T., Popov A., Iliev I., Stress induced birefringence in as-spun polyester fibers. *Journal of Optoelectronics and Advanced Materials – Symposia*, 2009, 1(3), 563 – 565.
- [7]. Bershtein V. A., Egorov V. M., Differential Scanning Calorimetry of Polymers, *Ellis Horwood Limited*, 1994, 256.



## ИЗИСКВАНИЯ КЪМ АВТОРИТЕ

В списание “Scientific and applied research” се публикуват на английски език кратки научни съобщения, отразяващи нови, непубликувани резултати от проучвания в областта на математическите, физическите, химическите, биологическите и медицинските науки, науките за Земята, инженерните, педагогическите и аграрните науки. Текстовете на статиите трябва да са подготвени за печат. Не се предвижда допълнително редактиране. Статиите се изпращат на адрес: zhekov\_z@abv.bg

Полетата на всяка страница трябва да са: ляво 25 mm, дясно 25 mm, горно 25 mm, долно 30 mm. На листа не се чертае рамка. На първа страница над заглавието да се оставят 60 mm (т.е. горно 25 + 35mm), на формат А4. Максималният обем на статиите е 8 страници. Студия се оформя както статия, в обем от 21 до 30 страници.

### УКАЗАНИЯ ЗА ОФОРМЯНЕ НА ТЕКСТА

**ЗАГЛАВИЕ** – Font: Times New Roman; Size: 14; Fontstyle: **Bold**; Effects: AllCaps; ParagraphAlignment: Centered.

**ИМЕНА НА АВТОРИТЕ** се печатат през 1 празен ред под заглавието в разгърнат вид - пълно собственои пълно фамилно име; Font: Times New Roman, Size: 14, Fontstyle: **Bold**, ParagraphAlignment: Left, по средата на реда – Centered.

**АНОТАЦИЯТА И КЛЮЧОВИТЕ ДУМИ НА АНГЛИЙСКИ ЕЗИК** се оформят така: Анотацията (**Abstract**:) в обем до 10 реда - Font: Times New Roman, Size: 12, Fontstyle: *Italic*, ParagraphAlignment: Justified; през 1 празен ред следват ключовите думи (дескриптори - **Keywords**) – Font: Times New Roman, Size: 12, Fontstyle: *Italic*; ParagraphAlignment: Justified, и двата елемента с отстъп 1 cm вляво от рамката, ограничаваща основния текст.

**ОСНОВЕН ТЕКСТ** – Font: Times New Roman, Size: 14; ParagraphFirstline: cm, Linespacing: Single, Alignment: Justified. Фигурите, с обяснителен текст, трябва да бъдат прецизно изработени и равномерно разположени върху страниците. Задължително е използването на международната система за мерните единици (SI). Чертежите, илюстрациите и снимките се обозначават в текста като фигури, съкратено „фиг.”. Те трябва да бъдат ясни и контрастни и да се придружават от текст. Приложените фигури и снимки да не са цветни.

Литературата в текста се означават с цифра, заградена в квадратни скоби [1] Номерацията на формулите се означават вляво от тях в малки кръгли скоби ( ). Литературата, посочена в края на доклада, се изписва съгласно стандарта за библиографско описание, на английски език а цитиранията в текста се означават с цифра, заградена в квадратни скоби [1].

Литературната справка трябва да съдържа не повече от 20 публикувани работи, цитирани в статията, подредени в хронологичен ред според цитирането им в текста. Името на първия автор се дава в инверсия. Следват съкратеното заглавие на списанието, том, година, книжка, страници (от - до), а при книги и монографии - заглавие, град, издателство, години, страници.

**АДРЕСИ ЗА КОРЕСПОНДЕНЦИЯ** се изписват през един празен ред (без абревиатури), Font: Times New Roman, Size: 12; Fontstyle: *Italic*; Effects: AllCaps, ParagraphAlignment: Justified, по средата на реда – Centered. Научни степени и звания, както и военни звания не се посочват.

Всяка статия се рецензира от двама независими анонимни рецензенти. След одобрение от рецензентите статията се приема за печат.



## REQUIREMENTS FOR THE AUTHORS

The journal “Scientific and applied research” publishes reports of original scientific results in the field of mathematical, physical, chemical, biological, medical, Earth and life sciences as well as engineering, pedagogical and agrarian sciences in English. The text papers should be styled for printing. No additional redaction is planned. The papers should be sent to the following address: zhekov\_z@abv.bg

The Fields on each page should be: left - 25 mm, right - 25 mm, top - 25 mm, bottom - 30 mm. No frame on sheet. On the first page under the title should be left 60 mm (top 25 + 35 mm), All papers shall be printed on a laser printer on standard sheets of paper format A4. The paper volume shall not exceed 8 pages. Each study should be styled as a paper in a volume of 21 to 30 pages.

### Text shall be styled in the following way

**TITLE** - Font: Times New Roman; Size: 14; Fontstyle: **Bold**; Effects: AllCaps; Paragraph Alignment: Centered.

**AUTHOR NAMES** - shall be printed over empty line under the title in its complete form – complete name, initial for the surname and complete family name; Font: Times New Roman, Size: 14, Fontstyle: **Bold**, Paragraph Alignment: Left, по средата на реда – Centered.

**ANNOTATION AND KEYWORDS IN ENGLISH** are styled as follows: annotation (ABSTRACT) in volume up to 10 lines - Font: Times New Roman, Size: 12, Fontstyle: *Italic*, Paragraph Alignment: Justified; the keywords are next over empty line (*descriptors* - **KEY WORDS**) – Font: Times New Roman, Size: 12, Fontstyle: *Italic*; Paragraph Alignment: Justified, both elements outstand 1 cm left of the frame limiting the main text.

**MAIN TEXT** - Font: Times New Roman, Size: 14; Paragraph Firstline: cm, Linespacing: Single, Alignment: Justified. **Drawings** shall be precise and evenly placed on pages. The International System of Units (SI) should be used. All graphs, illustrations and photographs are referred to as Figures, abbreviated to “Fig.”. They should be clear and contrasting and should be accompanied by text. The applied figures and pictures shouldn't be color.

The literature in the text should be denoted by a number in square brackets [1]. **Numbers of formulas** are printed on their left in brackets ( ).

**Literature**, stated at the end of the paper shall be printed according to the bibliographic description standard, and citations within the text are marked with a number in square brackets [<sup>1</sup>].

The references should contain up to 20 cited works arranged according to their order of appearance in the text. The family name precedes the initials of the first name in case of the first author. The references should include the names of the authors, followed by the standard abbreviation of the journal, the volume number, the year of publication, number of the journal and the pages cited. For books - the titles, the city of publication and the publisher followed by the year of publication and pages.

**MAILING ADDRESSES** printed over one more empty line (no abbreviations), Font: Times New Roman, Size: 12; Fontstyle: *Italic*; Effects: AllCaps, Paragraph Alignment: Justified, in the middle of the line – Centered.

Military and scientific degrees shall not be pointed.

All manuscripts submitted for publication must first be reviewed by two independent anonymous reviewers. After the approval of the manuscript by the reviewers the paper is submitted for publication.